OFFICE OF CIVILIAN RADIOACTIVE WASTE MANAGEMENT
CALCULATION COVER SHEET

1. QA: QA
Page: 1 Of: 66

2. Calculation Title

EQ6 Calculation for Chemical Degradation of Shippingport PWR (HEU Oxide) Spent Nuclear Fuel Waste Packages

3. Document Identifier (including Revision Number)

CAL-EDC-MD-000002 Rev 00

MOL.19991220.0322

4. Total Attachments	5. Attachment Numbers – Number of pages in each
4	I-1, II-4, III-3, IV-36 10 P.T. 12/2/99

	Print Name	Signature	Date
6. Originator	Sara Arthur	Sara Arthur	11-22-99
7. Checker	Kaveh Zarrabi	K. Zarrabi	11-24-99
8. Lead	Peter Gottlieb	Peter Gottlieb	12-2-99

9. Remarks

Attachment II is the list of the electronic file and their attributes contained in Reference 21.
Attachment IV is the Document Input Reference Sheets (DIRS).

Revision History

10. Revision No.	11. Description of Revision
00	INITIAL ISSUE

CONTENTS

FIGURES

Page

TABLES

1. PURPOSE

The Monitored Geologic Repository (MGR) Waste Package Operations (WPO) of the Civilian Radioactive Waste Management System Management & Operating Contractor (CRWMS M&O) performed calculations to provide input for disposal of spent nuclear fuel (SNF) from the Shippingport Pressurized Water Reactor (PWR) (Ref. 1). The Shippingport PWR SNF has been considered for disposal at the proposed Yucca Mountain site. Because of the high content of fissile material in the SNF, the waste package (WP) design requires special consideration of the amount and placement of neutron absorbers, and the possible loss of absorbers and SNF materials over geologic time. For some WPs, the corrosion-allowance barrier and the corrosion-resistant material (CRM) may breach (Refs. 1 and 2), allowing the influx of water. Water in the WP will moderate neutrons, increasing the likelihood of a criticality event within the WP; and the water may, in time, gradually leach the fissile components and neutron absorbers out of the WP, further affecting the neutronics of the system.

The purpose of this document is to present the simulation of long-term geochemical behavior of WPs containing Shippingport PWR SNF assemblies and high-level waste (HLW) glass canisters arranged according to the codisposal concept (Ref. 4). The specific objectives were to determine:

- The extent to which criticality control material, suggested for this WP design, will remain in the WP after corrosion/dissolution of the initial WP configuration (such that it can be effective in preventing criticality).

- The extent to which fissile plutonium and uranium will be carried out of the degraded WP by infiltrating water (such that internal criticality is no longer possible, but the possibility of external criticality may be enhanced).

- The nominal chemical composition for the criticality evaluations of the WP design, and to suggest the range of parametric variations for additional evaluations.

For the above purpose, the chemical compositions (and subsequent criticality evaluations) for some of the simulations are represented for time periods up to 6.342×10^5 years. This longer time frame is closer to the one million year time horizon recently recommended by the National Academy of Sciences to the Environmental Protection Agency for performance assessment related to a nuclear repository (Ref. 5). However, it is important to note that after 100,000 years most of the materials of interest (fissile and neutron absorber materials) will have either been removed from the WP, reached a steady state, or been transmuted.

The calculation included elements with high neutron-absorption cross sections, notably boron (B) as well as the fissile materials. The results of this calculation will be used to ensure that the type and amount of criticality control material used in the WP design will prevent criticality.

This document has been prepared according to Procedure AP-3.12Q/Rev. 0/ICN 0, Calculations, and is subject to the Quality Assurance Requirements and Description (QARD) Document (DOE/RW-0333P, Revision 08) requirements.

2. METHOD

The method used for this analysis involves the following steps:

- Use of basic EQ3/6 (software package, Section 4.1) capability for tracing the progress of reactions with evolution of the chemistry, which includes the estimation of the concentrations remaining in solution and the composition of the precipitated solids. (EQ3 is used to determine a starting fluid composition for EQ6 calculations; it does not simulate reaction progress).

- Evaluation of available data on the range of dissolution rates for the materials involved, to be used as material/species input for each time step.

- Use of "solid-centered flow-through" (SCFT) mode in EQ6; in this mode, an increment of aqueous "feed" solution is added continuously to the WP system, and a like volume of the existing solution is removed, simulating a continuously-stirred tank reactor. This mode is discussed in Section 4.

- Determination of fissile material concentrations in solution as a function of time (from the output of EQ6 simulated reaction times up to 6.342×10^5 years).

- Calculation of the amount of fissile material released from the WP as a function of time (fissile material loss reduces the chance of criticality event within the WP).

- Determination of concentrations of neutron absorbers, such as B, in solution as a function of time (from the output of EQ6 over times up to or somewhat greater than 6.342×10^5 years).

- Calculation of the amounts of neutron absorbers retained within the WP as a function of time.

- Determination of composition and amounts of solids (precipitated minerals or corrosion products, and unreacted WP materials).

Further detail on the specific methods employed for each step is available in Section 5 of this calculation.

3. ASSUMPTIONS

All assumptions are used throughout Section 5.

3.1 It is assumed that an aqueous solution fills all voids within WPs, and that the solutions that drip into the WP will have the composition of J-13 well water (as given in Ref. 6, Tables 4.1 and 4.2) for 6.342×10^5 years. The basis for the first part of this assumption is that it provides the maximum degradation rate with the potential for the fastest flushing of the neutron absorber out of the WP, and is thereby conservative. The basis for the second part of the assumption is that the groundwater composition is controlled largely by transport through the host rock, over pathways of hundreds of meters, and the host rock composition is not expected to change substantially over 10^6 years. For a few thousand years after waste emplacement the composition may differ because of perturbations resulting from reactions with engineered materials and from the thermal pulse. These are not taken into account in this calculation because the corrosion allowance barrier and CRM are not expected to breach until after that perturbed period. Therefore, the early perturbation is not relevant to the calculations reported in this document. See Assumption 3.3.

3.2 It is assumed that the density of the incoming water is 1.0 g/cm^3. The basis of this assumption is that in dilute solutions, the density is extremely close to that for pure water and that any differences are insignificant in respect to other uncertainties in the data and calculations. Moreover, this value is used only initially in EQ3/6 to convert concentrations of dissolved substances from parts per million to molalities.

3.3 The assumption that the water entering the WP can be approximated by the J-13 well water implicitly assumes: (1) that the infiltrating water will have only a minimal contact, if any at all, with unaltered metal in the corrosion allowance barrier, and (2) that any effects of contact with the drift liner will be minimal after a few thousand years. The basis for the first part of this assumption is that the water will move sufficiently rapidly through openings in the WP barriers that its residence time in the corroded barrier will be too short for significant reaction to occur. Furthermore, the water flowing through the barriers will be in contact with the corrosion products left from the barrier corrosion that created the holes in the first place, and these corrosion products will closely resemble iron oxides and hydroxides in the overlying rock. Consequently, the water should already be close to equilibrium with these compounds and would be unaffected by further contact with them, even if it flowed sufficiently slowly to permit significant reaction. The basis for the second part of this assumption is the following: (A) the drift liner at the top of the drift is expected to collapse with the roof support well before 1,000 years; and (B) the water flowing through the concrete liner, dominantly along fractures, will be in contact with the degradation products of the liner, which will have come close to equilibrium with the water moving through the rock above the repository. Interaction of water in the fractures with any unaltered concrete between fractures would be minimal

owing to the slow rate of diffusion through the matrix compared to rate of flow through fractures.

3.4 It is assumed that water may circulate sufficiently freely in the partially degraded WP that all degraded solid products may react with each other through the aqueous solution medium. The basis for this assumption is that this provides one bound for the extent of chemical interactions within the WP.

3.5 It is assumed that data in the 25 °C thermodynamic database can be used for the calculation. The basis for this assumption is that since the initial breach of the WP may occur when the WP contents are at temperatures ≥ 50 °C (Ref. 7, Figures 3-20 through 3-22), at times > 25,000 years, the WP temperatures are likely to be close to 25 °C.

3.6 In general it is assumed that chromium and molybdenum will oxidize fully to chromate (or dichromate) and molybdate, respectively. This assumption is based on the available thermodynamic data, which indicate that in the presence of air the chromium and molybdenum would both oxidize to the VI valence state. Laboratory observation of the corrosion of Cr and Mo containing steels and alloys, however, indicates that any such oxidation would be extremely slow. In fact, oxidation to the VI state may not occur at a significant rate with respect to the time frame of interest, or there may exist stable Cr (III) solids (not present in the EQ3/6 thermodynamic database) that substantially lower aqueous Cr concentration. For the present analyses, the assumption is made that over the times of concern oxidation will occur. This is conservative for times of several thousand years after WP breach, when the high pH solution from any drift liner effects will have been flushed out of the WP. Extreme acidification of the water will enhance solubility (Ref. 2) and transport of neutron absorber out of the WP thereby separating it preferentially from fissile material.

3.7 It is assumed that the CRM (the inner barrier) of the WP will react so slowly with the infiltrating water (and water already in the WP) as to have a negligible effect on the chemistry. The bases for this assumption consist of the facts that the CRM is fabricated from Alloy 22 (see nomenclature in Section 5.1.1), which corrodes very slowly compared (1) to other reactants in the WP and (2) to the rate at which soluble corrosion products will likely be flushed from the WP.

3.8 It is assumed that gases in the solution in the WP will remain in equilibrium with the ambient atmosphere outside the WP. In other words, it is assumed that there is sufficient contact with the gas phase in the repository to maintain equilibrium with the CO_2 and O_2 present, whether or not this be the normal atmosphere in open air or rock gas that seeps out of the adjacent tuff. Under these conditions the partial pressure of CO_2 exerts important controls on the pH and carbonate concentration in the solution and hence on the solubility of uranium and other elements. The basis for this assumption is that the measured composition of J-13 well water is not in equilibrium with the partial pressure of

CO_2 in the atmosphere (Ref. 8). By adjusting the average measured composition of the water slightly, well within the standard deviation of the measurements, it is possible to determine a partial pressure of CO_2 nearly ten times atmospheric (Ref. 8, Table 8; Ref. 9, p. F-210), with which this water was apparently in equilibrium at depth in the well. In another EQ6 calculation (Ref. 2), two runs with normal atmospheric CO_2 levels were used to determine the sensitivity of the calculations to this parameter. This high partial pressure is close to the maximum found by measurement of the rock gas composition (Ref. 8, Table 8). Therefore, this high partial pressure was chosen for all of the computer runs used in this analysis. The high CO_2 tends to increase the concentration of free carbonate ion and its complexation with the dissolved $U^{(VI)}$, thereby tending to increase the solubility of U, but this is moderated by the reduction of pH. There is little overall net effect on actinide solubility for otherwise comparable conditions.

3.9 It is assumed that precipitated solids are deposited, remain in place, and are not mechanically eroded or entrained as colloids in the advected water. The basis for this assumption is that since dissolved fissile material (U, Pu) may be adsorbed on colloids (clays, iron oxides) or precipitated as colloids during WP degradation (Ref. 7, Secs. 3.5 and 3.6), it is conservative, for internal criticality, to assume that all precipitated solids, including mobile colloids, will be deposited inside the WP rather than transported out of the WP.

3.10 It is assumed that corrosion rates will not be significantly enhanced by microbiologically influenced corrosion (MIC). The bases for this assumption are that: 1) MIC will probably not occur until the repository has cooled to temperatures below 100 °C (212 °F) and relative humidity is above 60%; 2) although MIC may increase corrosion pit and crevice density, its impact on corrosion rate will be low; and 3) Alloy 22 has not been associated with documented cases of MIC (Ref. 7, p. 3-84).

3.11 It is assumed that sufficient decay heat is retained within the WP over times of interest to cause convective circulation and mixing of the water inside the WP. The analysis that serves as the basis for this assumption is discussed in Reference 10, Attachment VI.

3.12 It is assumed that the reported alkalinity in analyses of J-13 well water corresponds to bicarbonate (HCO_3^-) alkalinity. Contributors to alkalinity in J-13 well water, in addition to bicarbonate, potentially include borate, phosphate, and silicate. However, at pH less than 9 the contribution of silicate will be small, and in any case the concentrations of all three of these components in J-13 well water are small. Fluoride or nitrate do not contribute to alkalinity unless a sufficiently low pH is reached. The basis for this assumption is the observation that the calculated electrical neutrality, using the assumption, is zero, within the analytical uncertainty, as it should be. The same assumption is implicitly made in (Ref. 6, Table 4.1, p. 4.2).

3.13 It is assumed that the rate of entry of water into, as well as the rate of egress from, a WP is equal to the rate at which water drips onto the WP. The basis for this assumption is that for most of the time frame of interest, i.e., long after the corrosion barriers become largely degraded, it is more reasonable to assume that all or most of the water will enter the degraded WP than to assume that a significant portion will instead be diverted around the remains. Diversion of the water with a consequent lower entry rate has not been represented by the present calculations.

3.14 It is assumed that the most insoluble solids for a fissile radionuclide will form, i.e., equilibrium will be reached. The basis for this assumption is to have a conservative approach for internal criticality because the assumption will lead to simulation of maximal retention of fissile material within the WP.

3.15 A number of minor assumptions have been made about the geometry of the Shippingport PWR codisposal WP. These assumptions are outlined and referenced in the spreadsheet ShipKL19sea.xls (Ref. 21), and are also discussed in Section 5.1. The bases for these assumptions are to represent the WP geometry with the greatest accuracy and, where inadequate information is available, to choose among competing representations of WP geometry, the choice that appears to lead to greatest conservatism is always made.

3.16 For any WP components that were described as "316" stainless steel, without indication of the carbon grade, the alloy was assumed to be the low-carbon equivalent (see Section 5.1.1 for nomenclature). The basis for this assumption is that, in general, the carbon in the steel is totally insignificant compared to the carbon supplied by the fixed CO_2 fugacity of the EQ3/6 calculation, and to the constant influx of carbonate via the incoming water. An underestimation of carbon in steel results in a slight overestimation of the remaining metals in the steel, which increases acid production very slightly and is therefore conservative.

3.17 Zircaloy and Zr corrosion kinetics studies (Ref. 11) revealed these materials to be resistant against chemical and biological corrosion. Recent studies on corrosion of Zircaloy-clad SNF indicate growth of oxide films for a time span of a million years to be about 7.6E-03 millimeter (0.3 mil). Since breach of the cladding would probably only occur as a result of mechanical damage or defect, most of the EQ6 cases were run with 1% and a few cases with 100% of the SNF surface area exposed to water (see Table 5-9). It was also assumed that the Zr cladding would breach soon after it comes in contact with water. Results from the EQ6 runs with 100% SNF surface area exposed to water had losses of U, Pu, and B similar to the cases run with only 1% SNF exposure (See Table 5-9). The bases for these assumptions are justified since they are conservative and account for any cladding that is damaged during storage, shipping, or packing.

4. USE OF COMPUTER SOFTWARE AND MODELS

This section describes the computer software used to perform the calculation.

EQ3/6 Software Package–The EQ3/6 software package originated in the mid-1970s at Northwestern University (Ref. 16). Since 1978, Lawrence Livermore National Laboratory (LLNL) has been responsible for maintenance of EQ3/6. The software has most recently been maintained under the sponsorship of the Civilian Radioactive Waste Management Program of the United States Department of Energy (DOE). The major components of the EQ3/6 package include: EQ3NR, a speciation-solubility code; EQ6, a reaction-path code, which represents water/rock interaction or fluid mixing in either a reaction-progress mode (independent of time) or a time mode; EQPT, a data file preprocessor; EQLIB, a supporting software library; and several (more than 5) supporting thermodynamic data files. The software deals with the concepts of thermodynamic equilibrium, thermodynamic disequilibrium, and reaction kinetics. The supporting data files contain both standard state and activity coefficient-related data. Most of the data files support the use of the Davies or B-dot equations for the activity coefficients; two others support the use of Pitzer's equations. The temperature range of the thermodynamic data in the data files varies from 25 °C only, for some species, to a full range of 0-300 °C for others. EQPT takes a formatted data file (a "data0" file) and writes an unformatted "data1" file, which is actually the form read by EQ3NR and EQ6. EQ3NR is useful for analyzing groundwater chemistry data, calculating solubility limits, and determining whether certain reactions are in states of partial equilibrium or disequilibrium. EQ3NR is also required to initialize an EQ6 calculation.

EQ6 represents the consequences of reacting an aqueous solution with a set of reactants, which react irreversibly. It can also represent fluid mixing and the consequences of changes in temperature. This code operates both in a reaction-progress frame (independent of time) and in a time frame. In a time frame calculation, the user specifies rate laws for the progress of the irreversible reactions. Otherwise, only relative rates are specified. EQ3NR and EQ6 use a hybrid Newton-Raphson technique to make thermodynamic calculations. This is supported by a set of algorithms that create and optimize starting values. EQ6 uses an ordinary differential equation (ODE) integration algorithm to solve rate equations in time mode. The codes in the EQ3/6 package are written in FORTRAN 77 and have been developed to run under the UNIX operating system on computers ranging from workstations to supercomputers. Further information on the codes of the EQ3/6 package is provided (Refs. 16, 17, 18, and 19).

Solid-Centered Flow-Through Mode–EQ6 Version 7.2b, as distributed by LLNL, does not contain an SCFT mode. To add this mode, it is necessary to change the EQ6 source code, and recompile the source. However, by using a variant of the "special reactant" type built into EQ6, it is possible to add the functionality of SCFT mode in a very simple and straightforward manner. This mode was added to EQ6 per Software Change Request (SCR) LSCR198 (Ref. 12), and the Software Qualification Report (SQR) for Media Identifier 30084-M04-001 (Ref. 13).

The new mode is induced with a "special-special" reactant. The EQ6 input file nomenclature for this new mode is jcode=5; in the Daveler format, it is indicated by the reactant type DISPLACER. The jcode=5 is immediately trapped and converted to jcode=2, and a flag is set to indicate the existence of the DISPLACER reactant. Apart from the input trapping, the distinction between the DISPLACER and SPECIAL reactants is seen only in one 9-line block of the EQ6 FORTRAN source code (in the reacts subroutine), where the total moles of elements in the rock plus water system (mte array) is adjusted by adding in the DISPLACER reactant, and subtracting out a commensurate amount of the total aqueous elements (mteaq array).

This new EQ6 mode acts as a substitute for the allpost/nxtinput method described in References 14 and 22.

4.1 SOFTWARE APPROVED FOR QUALITY ASSURANCE (QA) WORK

The software package, EQ3/6 Version 7.2b (Ref. 13) was used to provide the following:

- A general overview of the expected chemical reactions
- The degradation products from corrosion of the waste forms and canisters
- An indication of the minerals and their amounts likely to precipitate within the waste package.

The software specifications are as follow:

- Software name: EQ3/6
- Software version/revision number: Version 7.2b
- Software tracking number: UCRL-MA-110662 V 7.2b
- Computer type: personal computer (PC) (Ref. 15).

The input and output files attributes for the various EQ6 calculations are documented in Attachment II. The calculation files described in Sections 5 and 6 are such that an independent repetition of the software used may be performed.

The EQ3/6 software used was: (a) appropriate for the calculations performed, (b) used only within the range of validation as documented in Reference 13, and (c) obtained from the Software Configuration Management in accordance with appropriate procedures.

4.2 SOFTWARE ROUTINES

Spreadsheet analyses were performed with Microsoft Excel Version 97, installed on a PC. The specific spreadsheets used for results reported in this document are included in the electronic media (Ref. 21).

4.3 MODELS

None used.

5. CALCULATION

The existing database supplied with the EQ3/6 computer package is sufficiently accurate for the purpose of this calculation. The data have been carefully scrutinized by many experts over the course of several decades and carefully selected by LLNL for incorporation into the data base (Refs. 16, 17, 18, and 19). These databases are periodically updated and/or new databases added, such as one including extensive data on the lanthanides (Ref. 20). Every run of either EQ3 or EQ6 documents automatically which database is used. The databases include references internally for the sources of the data. The reader is referred to this documentation, included in the electronic files labeled data0 that accompany this calculation, for details (Ref. 21). Nevertheless, the quality of data needs to be verified in the future.

The calculations begin with selection of data for compositions, amounts, surface areas, and reaction rates of the various components of Shippingport PWR SNF WPs. These quantities are recalculated to the form required for entry into EQ6. For example, weight percentages of elements or component oxides are converted to mole fractions of elements; degradation rates in micrometers/year are converted into moles per square centimeter per second, etc. Spreadsheets (Ref. 21) provide details of these calculations, and the general procedure is also described in detail in Reference 22 (Section 4). The final part of the input to EQ6 consists of the composition of J-13 well water together with a rate of influx to the WP that corresponds to suitably chosen percolation rates into a drift and drip rate into a WP (Section 5.1.1.3). The EQ6 output provides the results of simulating of the chemical degradation of the WP, or components thereof. Sometimes the degradation of the WP is divided into phases, e.g., degradation of HLW glass before breach and exposure of the SNF assemblies and basket materials to the water. The results include the compositions and amounts of solid products and of substances in solution. Details of the results are presented below.

In all tables from this document, the number of digits reported does not necessarily reflect the accuracy or precision of the calculation. In most tables, two to four digits after the decimal place have been retained to prevent round-off errors in subsequent calculations.

5.1 CALCULATION INPUTS

5.1.1 WP Materials and Performance Parameters

This section provides a brief overview of the physical and chemical characteristics of Shippingport PWR SNF WPs, and describes how one is represented in the EQ6 inputs. The conversion of the WP physical description into parameters suitable for the EQ6 input files is performed by the spreadsheet *ShipKL19sea.xls*. Additional details of the description maybe found in References 1 and 2 and the references cited therein.

Material nomenclature used throughout this document includes: SA-240 S31603 (hereafter referred to as 316L), universal numbering system (UNS) N06625 and SA-240 S30403 (hereafter referred to as 304L), and SA-516 (hereafter referred to as A516).

5.1.1.1 Physical and Chemical Form of Shippingport PWR SNF WPs

It is convenient to consider the Shippingport PWR SNF WP as several structural components, specifically:

- The outer shell, consisting of the corrosion-allowance barrier and the CRM
- The "outerweb," a carbon steel (A516) structure designed to hold the HLW glass pour canisters (GPCs) in place
- The GPCs, the 304L containers of the solidified HLW glass
- The DOE SNF canister (sometimes called the "18-inch canister")
- The SNF assembly, exclusive of the SNF, a basket constructed of 316 L stainless steel plates and a spacer
- The individual SNF assemblies.

The details of each of the above numbered components are in the spreadsheet *ShipKL19sea.xls* in sheets "Fuel Wafers," "Poison, Cr, Inc-X," "Zirc-4 Clusters," "SNF Canisters," "Outer_Web," and "Glass_Canisters" (Ref. 21) and Reference 1 (Appendix C, pp. C-1 to C-18).

Table 5-1 provides a summary of the compositions of the principal steel alloys used in the calculations. Table 5-2 provides average and maximum degradation rates for the steels and the chrome plating. For a comparable specific surface area, the carbon steel is expected to degrade much more rapidly than the stainless steels (316L and 304L). In addition, the stainless steels contain significant amounts of Cr and Mo and, under the assumption of complete oxidation (Assumption 3.6), should produce more acid, per volume, than the carbon steel.

Table 5-1. Steel Compositions

	A516 Carbon Steel		304L Stainless Steel		316L Stainless Steel		304L with 2.33 wt% Natural Boron (0.43 wt% Boron-10)	
Element	wt%	Atom Fraction	wt%	Atom Fraction	wt%	Atom Fraction	wt%	Atom Fraction
C	0.30	0.0138	0.03	0.0014	0.03	0.0014	0.03	0.0012
Mn	1.03	0.0103	2.00	0.0199	2.00	0.0202	1.95	0.0178
P	0.04	0.0006	0.05	0.0008	0.05	0.0008	0.04	0.0007
S	0.04	0.0006	0.03	0.0005	0.03	0.0005	0.03	0.0005
Si	0.28	0.0054	0.75	0.0146	0.75	0.0148	0.73	0.0130
Cr			19.00	0.1997	17.00	0.1810	18.56	0.1782
Ni			10.00	0.0931	12.00	0.1132	9.77	0.0831
Mo					2.50	0.0144		
N			0.10	0.0039	0.10	0.0040	0.10	0.0035
Fe	98.33	0.9694	68.05	0.6660	65.55	0.6498	66.46	0.5943
B							2.33	0.1078
Total	100.00	1.0000	100.00	1.0000	100.00	1.0000	100.00	1.0000

Table 5-2. Steel Degradation Rates

	A516 Carbon Steel[a]	304L Stainless Steel[b]	316L Stainless Steel[b]	304L with 2.33 wt% Natural Boron (0.43 wt% Boron-10)[b]	Chrome Plating[b, c]
Molecular Weight (g/mol)	55.06	54.66	55.36	49.94	52.00
Density (g/cm^3)	7.85	7.94	7.98	7.94	7.2
Average Rate (μm/y)	35	0.1	0.1	0.1	0.1
Average Rate (mol/cm^2·s)	1.58E-11	4.61E-14	4.58E-14	4.61E-14	4.61E-14
High Rate (μm/y)	100	1	1	1	1
High Rate (mol/cm^2·s)	4.53E-11	4.61E-13	4.58E-13	4.61E-13	4.61E-13

SOURCES: [a] Reference 26, Figures 5.4-3, 5.4-4, and 5.4-5.
[b] Reference 23 (pp. 11-13).
[c] Reference 1 (Appendix C, Table C-3, pp. C-15 through C-18).

Table 5-3 gives the molar composition of the HLW glass used in the calculations (Ref. 24). The composition in Reference 24 was altered slightly to produce the values of weight percent listed in Table 5-3 (worksheet "glass" in spreadsheet "ShipKL19SEA.xls" in Ref. 21). The isotope ^{238}Pu was converted to ^{234}U; ^{241}Pu was converted to ^{237}Np; small amounts of neutron absorber (Th, Zn, and Ag) were removed to decrease the number of species; and small amounts of cesium were removed due to insufficient data on cesium in the EQ6 database. The numbers used in the column "Moles, Normalized" are used by EQ6 and represent the moles of each element in 100 grams of HLW glass.

The actual HLW glass composition used in the GPCs may vary significantly from the one given in Table 5-3 since the sources of the HLW glass and melting processes are not currently fixed. For example, compositions proposed for Savannah River Site HLW glass vary by a factor of ~6 in U_3O_8 content, from 0.53 to 3.16 wt% (Ref. 25, p. 3.3-15, Table 3.3.8.). The Si and alkali metal contents (Na, Li, and K) of the HLW glass have perhaps the most significant bearing on EQ6 calculations. The amount of Si in the HLW glass strongly controls the amount of clay that forms in the WP, and the Si activity controls the presence of insoluble uranium phases such as soddyite ($(UO_2)_2SiO_4 \cdot 2H_2O$). In the early stages of an EQ6 run, as the HLW glass degrades, the alkali metal content increases and the pH rises. The Si and alkali metal contents in Table 5-3 are typical for DOE HLW glasses (Ref. 24). Rates for HLW glass degradation were taken from Reference 26 (Figure 6.2-5), and normalized in spreadsheet shipKL19sea.xls, sheet "Rates" (Ref. 21). The high rate corresponds approximately to pH 9 at 70 °C, and the low rate to pH 8 at 25 °C.

Table 5-3. HLW Glass Composition, Density, and Degradation Rates

Element	Weight%[a]	Moles, Normalized[c]
O	4.452E+01	2.8079E+00
U	1.867E+00	7.9147E-03
Np	9.471E-04	4.0320E-06
Pu	1.480E-02	6.2417E-05
Ba	1.120E-01	8.2583E-04
Al	2.319E+00	8.6724E-02
S	1.287E-01	4.0512E-03
Ca	6.582E-01	1.6572E-02
P	1.398E-02	4.5548E-04
Cr	8.210E-02	1.5935E-03
Ni	7.308E-01	1.2565E-02
Pb	6.062E-02	2.9523E-04
Si	2.177E+01	7.8204E-01
Ti	5.934E-01	1.2507E-02
B	3.193E+00	2.9802E-01
Li	1.468E+00	2.1344E-01
F	3.167E-02	1.6824E-03
Cu	1.518E-01	2.4104E-03
Fe	7.349E+00	1.3280E-01
K	2.972E+00	7.6706E-02
Mg	8.201E-01	3.4052E-02
Mn	1.549E+00	2.8451E-02
Na	8.580E+00	3.7662E-01
Cl	1.153E-01	3.2808E-03
Total	9.909E+01	4.9010E+00
Density	(g/cm^3)	2.85
Low Rate	($g/m^2 \cdot d$)[b]	1E-04
	($mol/cm^2 \cdot s$)	1.1574E-15
High Rate	($g/m^2 \cdot d$)[b]	3E-02
	($mol/cm^2 \cdot s$)	3.4722E-13

SOURCES: [a] Reference 24, Attachment I, page I-7.
[b] Reference 26, Figure 6.2-5.
[c] Reference spreadsheet: pu_ceram.xls, sheets "Compositions" and "Rates."

NOTE: [c] Normalized to 1 mole = 100 g (^{239}Pu converted to ^{234}U, ^{241}Pu converted to ^{237}Np; small amounts of neutron absorbers [Th, Zn] and Cs were removed to decrease number of species).

Table 5-4 summarizes the assumed characteristics of the Shippingport PWR SNF. No fission product inventory was available, so the calculations used the composition of fresh (unirradiated) fuel. Use of fresh fuel is conservative since most fission products have significant neutron absorption cross sections, and the unirradiated fuel has a higher fissile content than partially spent fuel.

Table 5-4. Assumed Composition and Degradation Rates for Average Shippingport PWR SNF Wafers

Element	Mole Fraction
^{235}U	7.1737E-02
^{238}U	5.2340E-03
Ca	5.2516E-02
Zr	2.2135E-01
O	6.4916E-01
Sum	1.0000E+00
Average Molecular Weight (UO_2, CaO, ZrO_2)	50.79
Average Density of SNF Wafers (g/cm^3)	5.80
Low SNF Degradation Rate (mg/m^2·d)	0.05
Low SNF Degradation Rate (mol/cm^2·s)	1.1394E-15
Moderate SNF Degradation Rate (mg/m^2·d)	1
Moderate SNF Degradation Rate (mol/cm^2·s)	2.2788E-14
High SNF Degradation Rate (mg/m^2·d)	30
High SNF Degradation Rate (mol/cm^2·s)	6.83643E-13

SOURCES: Reference 1 (Table C-2, pp. C-6 to C-14) and Reference 21 (Spreadsheet: ShipKL19_sea.xls, sheets "Fuel Wafers," and "Rates").

The outer web (Attachment I) is composed of A516 carbon steel, and serves two purposes: it centers and holds in place the DOE SNF canister; and it separates the GPCs and prevents them from transmitting undue stress to the SNF canister in the event of a fall (tip-over) of the entire WP. At the center of the outer web is a thick (3.175 cm) cylindrical support tube, also constructed of A516. In a breach scenario, the outer web will be exposed to water and corrosion before the rest of the WP, and is expected to degrade within a few hundred to a few thousand years. The oxidation of iron in the outer web steel into hematite (Fe_2O_3) can decrease the void space in the WP by ~13%, while iron transformation to goethite (FeOOH) can decrease the void space by ~22% (Ref. 2) since goethite has a larger molar volume than hematite (Table 5-10). Thus the void space can be significantly reduced, soon after breach of the WP, by the alteration of the outer web.

The DOE SNF canister fits inside the central support tube of the outer web. The canister is composed primarily of 316L, with two internal, thick impact plates of carbon steel (approximated as A516 in the calculations). A basket structure constructed of 316L stainless steel plates is located within the DOE SNF canister to maintain the position of the assembly in the center of the canister.

5.1.1.2 Chemical Composition of J-13 Well Water

It was assumed that the water entering the WP would have the same composition as that of water from the J-13 well (Assumptions 3.1 and 3.3). This water has been analyzed repeatedly over a span of at least two decades (Ref. 6). Tables 5-5 and 5-6 contain the EQ3NR input file constraints for J-13 well water composition and the EQ6 input file elemental molal composition for J-13 well water used for this calculation.

The "Basis Species" column of Table 5-5 lists the chemical species names recognized by EQ3NR and EQ6. Some of the components of J-13 well water, as analyzed (Ref. 6), are in a different chemical form than the species listed in this column; these components must be substituted or "switched" with the basis species for input into EQ6 and are listed in the "Basis Switch" column. Basis species listed as "Trace" in the "Basis Switch" column are not found in J-13 well water, as analyzed (Ref. 6), but must be input at a minimum concentration for numerical stability in EQ6 calculations.

Table 5-5. EQ3NR Input File Constraints for J-13 Well Water Composition

Basis Species	Basis Switch	Concentration	Units
redox		-0.7	log fO_2
Na+		4.580E+01	mg/l
SiO_2(aq)		6.097E+01	mg/l
Ca++		1.300E+01	mg/l
K+		5.040E+00	mg/l
Mg++		2.010E+00	mg/l
Li+		4.800E-02	mg/l
H+		8.1	pH
HCO_3-	CO_2(g)	-3	log fCO_2
O_2(aq)		5.600E+00	mg/l
F-		2.180E+00	mg/l
Cl-		7.140E+00	mg/l
NO_3-	NH_3(aq)	8.780E+00	mg/l
SO_4--		1.840E+01	mg/l
$B(OH)_3$(aq)		7.660E-01	mg/l
Al+++	Diaspore	0	Mineral
Mn++	Pyrolusite	0	Mineral
Fe++	Goethite	0	Mineral
HPO_4--		1.210E-01	mg/l
Ba++	Trace	1.000E-16	Molality[a]
CrO_4--	Trace	1.000E-16	Molality[a]
Cu++	Trace	1.000E-16	Molality[a]
Gd+++	Trace	1.000E-16	Molality[a]
MoO_4--	Trace	1.000E-16	Molality[a]
Ni++	Trace	1.000E-16	Molality[a]
Np++++	Trace	1.000E-16	Molality[a]
Pb++	Trace	1.000E-16	Molality[a]
Pu++++	Trace	1.000E-16	Molality[a]
TcO_4-	Trace	1.000E-16	Molality[a]
$Ti(OH)_4$(aq)	Trace	1.000E-16	Molality[a]
UO_2++	Trace	1.000E-16	Molality[a]
$Zr(OH)_2$++	Trace	1.000E-16	Molality[a]

NOTE: [a]The concentration of 1.0E-16 is added as a trace to ensure numerical stability.
SOURCE: Reference 6.

Table 5-6. EQ6 Input File Elemental Molar Composition for J-13 Well Water

Element	Mol/kg	Element	Mol/kg
O	5.55E+01	Mg	8.27E-05
Al	2.55E-08	Mn	3.05E-16
B	1.24E-05	Mo	1.00E-16
Ba	1.00E-16	N	1.42E-04
Ca	3.24E-04	Na	1.99E-03
Cl	2.01E-04	Ni	1.00E-16
Cr	1.00E-16	Np	1.00E-16
Cu	1.00E-16	Pb	1.00E-16
F	1.15E-04	Pu	1.00E-16
Fe	3.60E-12	S	1.92E-04
Gd	1.00E-16	Si	1.02E-03
H	1.11E+02	Tc	1.00E-16
C	2.09E-03	Ti	1.00E-16
P	1.26E-06	U	1.00E-16
K	1.29E-04	Zr	1.00E-16
Li	6.92E-06		

SOURCE: Reference 6.

5.1.1.3 Drip Rate of Water into a WP

It is assumed (Assumption 3.13) that the drip rate onto a WP is the same as the rate at which water flows through the WP. The drip rate is taken from a correlation between percolation rate and drip rate (Ref. 28, Tables 2.3-49 and 2.3-50). Specifically, percolation rates of 40 mm/y and 8 mm/y correlate with drip rates onto the WP of 0.15 m^3/y and 0.015 m^3/y, respectively. The choice of these particular percolation and drip rates is discussed in detail in Reference 22 (Section 5.1.1.3, p. 19).

For the present study, the range of allowed drip rates was extended to include an upper value of 0.5 m^3/y and a lower value of 0.0015 m^3/y. The upper value corresponds to the 95 percentile upper limit for a percolation rate of 40 mm/y, and the lower value is simply $1/10^{th}$ the mean value for the percolation rate of 8 mm/y (Ref. 28, Figure 2.3-108). These extreme values were used, because prior studies (Ref. 29, p. 28; Ref. 30, p. 5-19) suggested that when waste forms are codisposed with HLW glass, significant removal of a number of elements occurs when: (1) initial high drip rates cause HLW glass leaching and removal of alkali; and (2) subsequent low drip rates allow acid to build from steel degradation.

5.1.1.4 Calculation of Evaporated Salts Composition

The purpose of this calculation was to provide an estimate of the solids that might precipitate in the cruciform space within the Shippingport SNF assembly. The concern was that the precipitated salts would displace either air or water, substantially changing the neutron moderating properties of the cruciform. The composition of J-13 well water, as used for the Shippingport EQ6 runs, was numerically "evaporated," precipitating minerals in a sequence that assured charge balance. The results are given in Table 5-7. The details of the calculation are given in spreadsheet j13evaporIIK3.xls, included with the electronic media (Ref. 21).

Table 5-7. Moles, Grams, and Densities of Salts from Evaporated J-13 Well Water

Mineral	Amount of Salt (mol/l)	Amount of Salt (g/l)	Density (g/cm^3)
AlO(OH)	2.553E-08	1.531E-06	3.40
$Ca_2B_6O_{11}:5H_2O$	2.065E-06	8.488E-04	2.42
$CaCO_3$	1.287E-04	1.288E-02	2.71
KF	1.147E-04	6.666E-03	2.48
KCl	1.416E-05	1.056E-03	1.98
Li_2O	3.458E-06	1.033E-04	2.01
$MgCO_3$	8.270E-05	6.973E-03	2.96
NaCl	1.872E-04	1.094E-02	2.17
$Na_2CO_3:H_2O$	9.025E-04	1.119E-01	2.25
$CaSO_4$	1.915E-04	2.608E-02	2.96
SiO_2	1.015E-03	6.097E-02	2.32

5.1.1.5 Densities and Molecular Weights of Solids

For input to criticality calculations, one must convert moles of solids to volume of solids. A few solid phases contribute the overwhelming bulk of the total volume; Table 5-8 provides some of the densities and molar volumes for these phases. The current version of EQ6 (Section 4) performs the volume calculations for each element automatically.

Table 5-8. Densities and Molecular Weights of Precipitated Solids

Solid	Density (kg/m^3)	Molecular Weight (g/mol) [c]	Molecular Volume (cm^3/mol) [c]	Calculated Density (g/cm^3)
Diaspore (AlOOH)	3400[a]	59.988	17.760	3.378
Hematite (Fe_2O_3)	5240[b]	159.692	30.274	5.275
Pyrolusite (MnO_2)	5060[a]	86.937	17.181	5.060[a]
Goethite (FeOOH)		88.854	20.820	4.268
Ni_2SiO_4		209.463	42.610	4.916
Trevorite ($NiFe_2O_4$)		234.382	44.524	
Nontronite-Ca		424.293	131.100	3.236
Nontronite-K		430.583	135.270	3.183
Nontronite-Mg		421.691	129.760	3.250
Nontronite-Na		425.267	132.110	3.219

SOURCES: [a] Reference 31, p. 172.
[b] Reference 9, p. B-121.
[c] Reference 21 (EQ3/6 Data base, data0.nuc.R8a), g/mol, except for pyrolusite, which is calculated from the density and molecular weight. Trevorite given same molar volume as magnetite in EQ6 database.

5.1.1.6 Atomic Weights

Atomic weights were taken from References 32 (pp. 29-31) and 33 (Chart of the Nuclides), and are listed in Reference 21 (spreadsheet ShipKL19sea.xls, sheet "Atomic Weights").

5.2 DATA CONVERSION

The data presented in Section 5.1 are not in a form suitable for entry into EQ3/6. The transformation to EQ3/6 format involves converting mass fractions to mole fractions; normalizing surface areas, volumes, and moles to 1 liter reactive water in the system; and converting rates to $mol/cm^2 \cdot s$. Most of these conversions are straightforward and are performed in the spreadsheets, which are included in the electronic media for this document (Ref. 21). Reference 22 (Section 4) describes the conversion process in detail.

5.3 EQ6 CALCULATIONS AND SCENARIOS REPRESENTED

The rationale for selection of scenarios in EQ6 simulations is to provide conservative assessments of solubility and transport of fissile materials (i.e., U compounds) and neutron absorber species (i.e., B) in the WP. Uranium carbonate complexes form at high pH and might cause an increase in solubility of uranium. The *Disposal Criticality Analysis Methodology Topical Report* document defines the internal and external degradation scenarios for disposal criticality analysis (Ref. 34, pp. 3-9 through 3-12). The internal degradation configurations are based on the assumption that groundwater drips onto the upper surface of the WP and penetrates

it. Groundwater accumulates inside the WP and can dissolve and flush either neutron absorber or the SNF out of the WP. Following is a summary of three groups of degradation configurations from Reference 34:

- WP internals degrade faster than the waste forms.
- WP internals degrade at the same rate as the waste forms.
- WP internals degrade slower than the waste forms.

The WP internals include all components within the WP including neutron absorber materials (boron) except SNF. The waste forms refer to SNF. The above configurations set the framework in which EQ6 scenarios could be developed. The scenarios are based on sequence of chemical reactions as function of time and can be divided into two general categories: single-stage cases and multiple-stage cases.

Single-Stage Cases–In these calculations all WP internals, including SNF, come in contact with groundwater simultaneously. These cases correspond to an extreme in which the zirconium cladding is breached immediately, thereby exposing all or a portion of the SNF as soon as the WP corrosion barriers are breached. These cases result in the highest dissolved radionuclide levels, and might provide the most conservative estimate of fissile material and neutron absorber loss.

Multiple-Stage Cases–These EQ6 calculations start with the breach of WP allowing groundwater to come in contact with WP internals outside the DOE SNF canister ("stage A"); during this stage, the DOE SNF canister remains intact. The second stage ("stage B") starts with the breach of DOE SNF canister and interaction of groundwater with material inside DOE SNF canisters, as well as waste forms and unaltered reactants remaining from stage A. These cases were designed to produce the lowest possible pH, by first exposing the HLW glass to incoming water to remove alkalinity, prior to exposure of the SNF in the second stage.

In total, 30 cases of single- and multiple-stage EQ6 simulations, with different degradation rates of steel and HLW glass and different water fluxes through the WP, were run. These cases are discussed in the following sections.

5.3.1 EQ6 Run Conditions and Nomenclature

The EQ6 codes were used to run the 30 cases summarized in Table 5-9. In general each case could be classified as single or multiple stage. Cases 1-20 and 25-30 are single-stage, and involve simultaneous exposure of the SNF and the WP materials to groundwater. Considering that the SNF wafers are within zirconium cladding, for a conservative approach, it was assumed (Assumption 3.17) that cladding is fully breached immediately after contact with water. Cases 25 through 27 were done to consider the effect of the degree of SNF exposure on reaction. Case 28 was done to determine if the alteration product density depended on the identity of the iron oxide

that formed – hematite or goethite. This case was just a first stage, with hematite suppressed (with goethite), run to the same ending time and rates as the first-stage run (s03a2204), wherein hematite was allowed to form. Cases 29 and 30 were specifically done to assess the relative contribution of U from dissolving SNF and HLW glass.

Cases 21 through 24 are multiple-stage runs in which groundwater first interacts with everything inside the WP except the SNF canister, followed in the second stage by interaction of the resulting fluids with the SNF. It is also assumed that zirconium cladding would breach just after the breach of the DOE SNF canister.

The "Root File Names" column in Table 5-9 gives the root file names used to describe the runs. The EQ6 input files corresponding to these runs end with the extension ".6i" (e.g., s01a1131.6i is the EQ6 input file name for Case 3); these input files are included with the electronic media accompanying this calculation (Ref. 21). Each EQ6 run has associated tab-delimited text files, also included in the electronic media (e.g., s01a1131.elem_aqu.txt for Case 3). Several input files, corresponding to separate EQ6 runs, may be grouped into a "Case." Most of the important run conditions could be inferred from the root file name. Evaluation of root file names for most cases from left to right is as follows:

The first letter "s" corresponds to Shippingport.

The second and third characters (first and second digits after "s") correspond to revision of input file; for each case, the numbers range from 00 to 99. There are two exceptions. Those containing an "!" were done assuming 100% SNF exposure. Those containing an "@" were done using U-free HLW glass compositions.

The fourth character may correspond to stage number in multiple-stage runs (e.g., "a," "b") or to revisions of single-stage runs. Single-stage runs that do not converge usually require ("stage a") removal of the exhausted reactants and restart of the run. Each step is identified as a, b, c, etc. Some cases run with hematite suppressed have "g" as the fourth character.

The fifth digit is 1 or 2, corresponding to the average or high rates of steel corrosion in Table 5-1.

The sixth digit in this block is 1, 2 or 0, with 1 and 2 corresponding to the low and high HLW glass corrosion rates listed in Table 5-2, respectively, and 0 corresponding to no HLW glass present in the EQ6 run.

The seventh digit in the block is 1, 2, 3, or 0, with 1 corresponding to low rates of SNF dissolution, 2 corresponding to average dissolution rates, 3 corresponding to high dissolution (see Table 5-3), and 0 corresponding to no SNF present in the EQ6 run.

The last digit in the block encodes the choice of flush rate of the incoming water, with 1, 2, 3, and 4 corresponding to 0.0015 m^3/y, 0.015 m^3/y, 0.15 m^3/y, and 0.5 m^3/y, respectively.

Hematite and goethite are major iron-oxide minerals observed to form in rust, though the EQ6 thermodynamic database indicates hematite is thermodynamically more stable, and hematite's stability increases with temperature. An EQ6 simulation, in which the second letter (from left) of the file's root name is "g," indicates that formation of hematite in that run was suppressed. All the other characters in the root name are the same as those runs in which hematite was not suppressed.

5.3.2 Examination of Cases

Table 5-9 summarizes all the cases run, as well as total percentage of B, U, and Pu loss at the end of the EQ6 runs. The complete output tables (aqueous, mineral, and total moles) for all the cases are included in the electronic media, as text files (Ref. 21). A summary of the files included in the electronic media is given in Attachment II.

Tables 5-9 through 5-24 and Figures 5-1 through 5-4 illustrate the limits of system behavior. Specifically, single-stage runs show B, U, and Pu loss from the SNF and HLW glass to alteration products and solution as a function of reaction time, and how each output varies depending upon input steel corrosion rates, HLW glass corrosion rates, SNF corrosion rates, and fluid flow rates. The multiple-stage runs provide information on how the system might behave under a number of extreme scenarios. Cases 1-10 involve average steel degradation rates. Cases 11-20 entail high steel degradation. Examination of the results in Table 5-9 reveals the following generalizations about B, U, and Pu release from the WP:

- B loss is complete except when HLW glass dissolution rates are low and water fluxes are high.

- U and Pu losses are greatest when HLW glass dissolution rates are high. At a given HLW glass dissolution rate, U loss varies inversely with the flux of water, as does Pu loss. Steel corrosion and SNF degradation are third-order controls over U and Pu release.

Table 5-9. Summary of Cases Run; Associated Input File Names; Percent SNF Exposed; Percent B, Pu, and U Loss; and Fe Oxide Corrosion Product

Case ID	Root File Names	% SNF Exposure	%B Loss	%Pu Loss	%U Loss	Fe Oxide
1	s01a1111	1	100	12.3	100	hematite
2	s01a1113	1	16.2	0.09	0.06	hematite
3	s01a1131	1	100	12.3	100	hematite
4	s01a1133	1	16.3	0.10	0.06	hematite
5	s01a1122	1	100	1.28	100	hematite
6	s01a1211	1	100	100	94.5	hematite
7	s01a1213	1	100	41.2	100	hematite
8	s01a1231	1	100	100	94.5	hematite
9	s01a1233	1	100	41.2	100	hematite
10	s01a1222	1	100	100	100	hematite
11	s01a2111	1	100	7.68	100	hematite
12	s01a2113	1	16.2	1.50	0.24	hematite
13	s01a2131	1	100	7.68	100	hematite
14	s01a2133	1	16.9	1.50	0.31	hematite
15	s01a2122	1	100	1.84	100	hematite
16	s01a2211	1	100	66.3	100	hematite
17	s01a2213	1	100	55.3	100	hematite
18	s01a2231	1	100	66.3	100	hematite
19	s01a2233	1	100	55.3	100	hematite
20	s01a2222	1	100	99.9	100	hematite
21	s03a2204/s03b2022	1	99.5	31.7	100	hematite
22	s04a2204/s04b2022[a]	1	99.5	74.6	100	goethite
23	s02g2203/s02g2021[a]	1	99.5	0	24.2	goethite
24	s02g1203/s02g1021[a]	1	99.5	0	100	goethite
25	sl1a1113	100	16.2	0.09	0.07	hematite
26	sl1a1133	100	16.4	0.14	0.08	hematite
27	sl2g2021[a]	100	99.5	0	4.60	goethite
28	s04c2204[a,b]	0				goethite
29	s@1a1111[c]	1	100	12.7	100	hematite
30	s@1a1222[c]	1	100	100	100	hematite

NOTES: [a] These cases were run with hematite suppressed.
[b] This case was run with the same ending time as s03a2204.
[c] These cases were run with U removed from the HLW glass composition.

The general trend of iron-oxide corrosion product accumulation seen in Figure 5-1 is that iron oxides accumulate until roughly 100 years have elapsed, followed by either a plateuing of accumulation after about 250 years (e.g., runs s01a1111, s01a1133, s01a1222, s02g1203, s02g1021), or a quantitative decrease in total iron oxide after about a hundred years (e.g., runs s04a2204, s04b2022, s01a2233). The first group accumulated iron oxides slowly, in part, because steel corrosion rates were low, preventing accumulation of corrosion products. The second group accumulated iron oxides rapidly because higher steel degradation rates were used as input. The plateauing of iron-oxide accumulation in the first group, and the decrease in iron-oxide accumulation in the second group, arose because of the rapid, parallel increase in Fe-containing smectite (see Figure 5-2), which formed at the expense of, respectively, potentially new, and existing corrosion products.

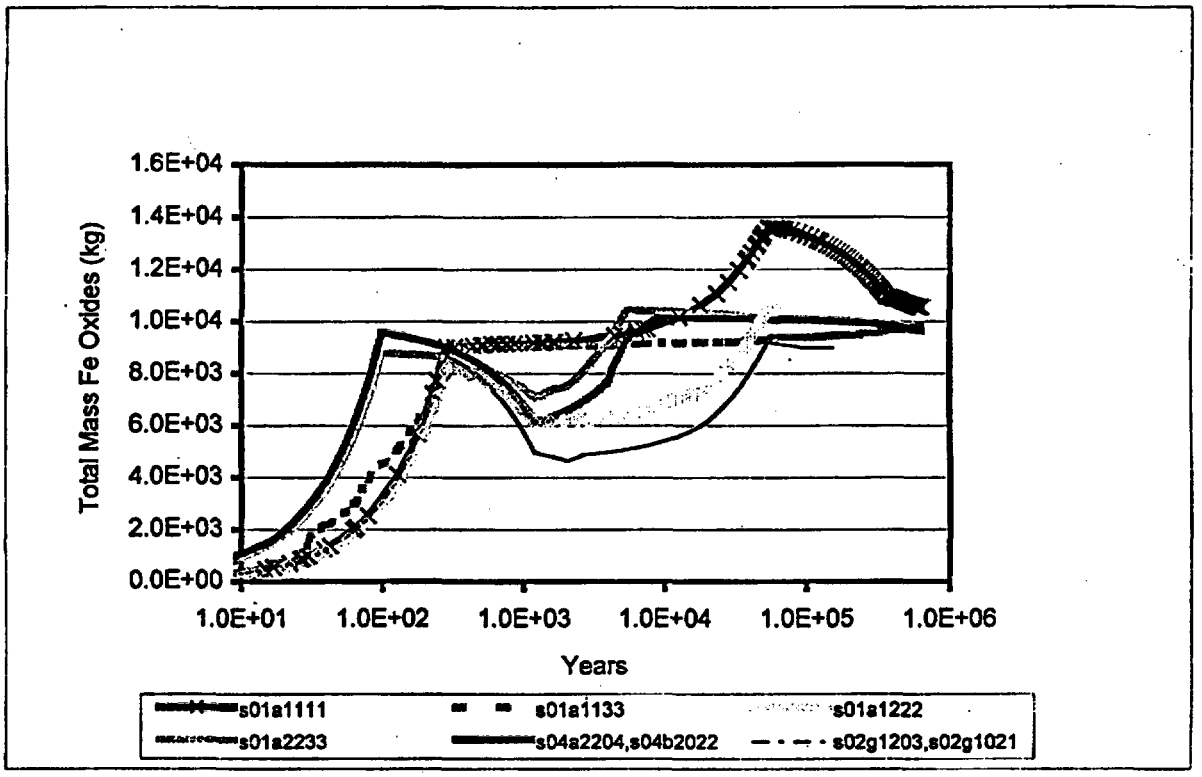

Figure 5-1. Predicted Accumulation of Iron-Oxide Degradation Products Over Time

Smectite accumulation as a function of time (Figure 5-2) likewise shows two types of behavior. Only minor amounts of smectite accumulate in the first 10,000 years in some runs (e.g., s01a1111 and s01a1133), while in others smectite accumulation becomes significant by 100 years, ultimately plateauing at roughly 1,000 years. The runs in which smectite formed late are runs in which pH was acidic for the first several thousand years of reaction. Smectites are more stable at neutral to high pH and are less likely to form under mildly acidic conditions. The runs where smectite formed early are those runs that were initially neutral to alkaline, or became neutral to alkaline early in the runs.

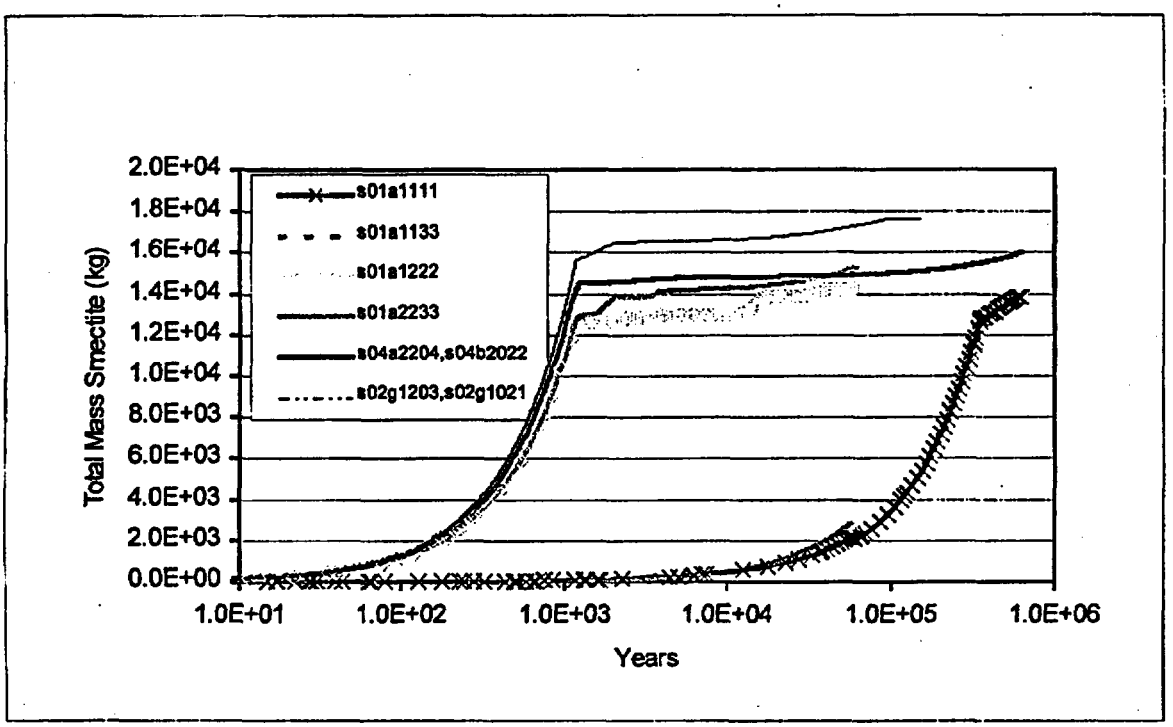

Figure 5-2. Predicted Accumulation of Smectite Degradation Products Over Time

Tables 5-10 and 5-11 show, respectively, elemental composition of alteration products and concentrations of dissolved species under conditions of average steel corrosion, low HLW glass corrosion, low SNF corrosion, and minimal flow rates (0.0015 m^3/y) – case s01a1111. Low flow rates, in particular, allow the buildup of solution acidity (note elevated Cr and Mo levels of Table 5-11) in the early stages of reaction. Solution pH in the WP remains below 6 for over 26,000 years, leading to low C and U levels in solution. Both tend to rise later due to carbonate complexation of uranyl under more alkaline conditions. Silicon levels remain reasonably constant over time at, or immediately below, quartz saturation (10^{-4} moles/l at near neutral pH, 25 °C). Boron, the primary neutron absorber present, remains at uniformly high solution concentrations ($10^{-2.3}$ to $10^{-1.1}$ moles/l, Table 5-11) throughout all but the last portion of the WP degradation process. Corrosion product amounts are listed as a function of time elapsed in Table 5-10. Note first of all that the bulk of degradation products consist of hematite, followed by Al and Si in smectites (Nontronites). Mn forms pyrolusite (MnO_2) in this, and many of the other, runs. Pu forms PuO_2 as an alteration phase, particularly towards the end of the run. U deposition, in the form of soddyite, is primarily confined to the first 30,000 years of reaction, though U is remobilized completely by the carbonate-rich, alkaline solutions that ultimately form. Net Pu loss is 12.3%. B loss is complete.

Table 5-10. Elemental Composition of Corrosion Products (mole%) and Density for Case 1 (s01a1111)

Time (y) / Element	282	6962	26652	122490	634220
O	6.01E+01	6.00E+01	5.99E+01	5.98E+01	5.94E+01
Al	2.48E-03	8.23E-02	2.41E-01	6.95E-01	1.25E+00
B	0.00E+00	0.00E+00	7.44E-15	0.00E+00	2.78E-15
Ba	3.58E-05	7.84E-04	2.29E-03	6.62E-03	1.19E-02
Ca	0.00E+00	1.43E-02	3.84E-02	1.27E-01	2.60E-01
Cl	0.00E+00	8.28E-14	0.00E+00	4.46E-14	0.00E+00
Cr	1.14E-05	1.06E-03	3.11E-03	1.71E-15	0.00E+00
Cu	0.00E+00	4.62E-04	2.15E-03	1.38E-02	3.11E-02
F	0.00E+00	2.11E-03	5.93E-03	7.51E-03	6.10E-03
Fe	3.91E+01	3.76E+01	3.45E+01	2.70E+01	1.81E+01
H	4.15E-02	5.03E-01	1.25E+00	3.01E+00	6.32E+00
C	0.00E+00	8.38E-14	0.00E+00	1.32E-01	2.36E-01
P	2.39E-02	2.23E-02	2.34E-02	2.25E-02	1.83E-02
K	0.00E+00	2.67E-02	6.76E-02	3.25E-01	6.06E-01
Li	0.00E+00	2.53E-12	0.00E+00	1.08E-01	0.00E+00
Mg	0.00E+00	1.31E-02	2.98E-02	1.91E-01	4.47E-01
Mn	4.18E-01	4.74E-01	5.86E-01	6.80E-01	6.93E-01
Mo	1.20E-19	2.54E-18	0.00E+00	0.00E+00	1.15E-31
N	0.00E+00	1.07E-12	0.00E+00	2.54E-18	0.00E+00
Na	0.00E+00	1.97E-02	4.55E-02	2.52E-01	1.12E-01
Ni	0.00E+00	2.32E-01	7.44E-01	1.01E+00	7.48E-01
Np	0.00E+00	4.61E-14	0.00E+00	0.00E+00	0.00E+00
Pb	1.14E-05	2.80E-04	8.19E-04	2.37E-03	4.27E-03
Pu	0.00E+00	0.00E+00	2.46E-14	3.52E-04	7.92E-04
S	3.58E-05	3.12E-11	0.00E+00	2.68E-12	0.00E+00
Si	2.56E-01	9.98E-01	2.49E+00	6.60E+00	1.16E+01
Tc	0.00E+00	0.00E+00	2.94E-31	0.00E+00	2.16E-32
Ti	5.44E-04	1.19E-02	3.47E-02	1.00E-01	1.81E-01
U	2.65E-05	7.51E-03	2.20E-02	0.00E+00	6.93E-25
Zr	2.19E-06	4.79E-05	1.40E-04	4.04E-04	2.52E-04
Total	100%	100%	100%	100%	100%
Total (kg)	8357	9329	11911	17397	24617
Density (g/cm^3)	5.26	5.17	5.01	4.48	3.88

Table 5-11. Solution Composition (mol/kg) in Selected Years for Case 1 (s01a1111)

Time (y) / Element / pH	282	6962	26652	67906	122490	634220
pH	2.48	5.71	5.71	8.82	9.42	8.61
Al	5.69E-04	1.67E-08	1.18E-08	9.29E-08	4.91E-08	8.43E-08
B	5.81E-03	6.86E-02	8.07E-02	8.07E-02	8.07E-02	1.24E-05
Ba	7.27E-08	1.40E-07	1.35E-07	5.81E-10	5.29E-11	6.12E-10
Ca	6.41E-04	7.76E-04	1.18E-03	4.52E-05	8.40E-06	3.56E-05
Cl	2.64E-04	9.48E-04	1.09E-03	1.09E-03	1.09E-03	2.01E-04
Cr	1.64E-02	1.82E-01	2.15E-01	5.16E-03	4.32E-04	1.00E-16
Cu	4.58E-05	4.12E-04	4.16E-04	9.01E-07	8.60E-06	3.86E-07
F	1.47E-04	1.36E-06	1.71E-07	5.23E-04	5.30E-04	1.14E-04
Fe	3.82E-06	8.55E-12	8.47E-12	1.38E-12	2.10E-12	1.27E-12
C	3.35E-05	4.29E-05	4.31E-05	7.08E-02	8.00E-02	7.05E-03
P	5.19E-04	1.37E-04	1.53E-04	1.58E-07	3.46E-06	2.74E-08
K	1.59E-03	1.12E-02	1.47E-02	4.63E-03	7.20E-03	2.38E-03
Li	4.06E-03	4.86E-02	5.78E-02	3.79E-02	5.72E-02	6.92E-06
Mg	7.30E-04	4.87E-03	6.66E-03	4.76E-05	6.66E-06	3.85E-05
Mn	7.27E-05	3.48E-11	3.42E-11	4.15E-16	1.40E-15	2.41E-16
Mo	2.55E-04	3.05E-03	3.62E-03	1.32E-05	3.18E-12	1.00E-16
N	4.48E-04	3.78E-03	4.44E-03	2.16E-04	1.42E-04	1.42E-04
Na	9.15E-03	8.30E-02	9.98E-02	9.13E-02	9.52E-02	5.51E-03
Ni	7.46E-03	3.00E-02	3.00E-02	2.03E-08	1.19E-09	2.29E-08
Np	7.67E-08	9.17E-07	1.09E-06	1.09E-06	1.09E-06	1.00E-16
Pb	6.38E-07	2.47E-10	2.40E-10	3.68E-10	2.09E-11	3.66E-10
Pu	1.19E-06	1.43E-05	1.69E-05	3.76E-09	5.45E-07	1.14E-11
S	1.09E-02	3.43E-03	1.86E-03	1.30E-03	1.29E-03	1.92E-04
Si	1.87E-04	5.37E-05	5.26E-05	4.16E-05	7.30E-05	3.63E-05
Ti	2.26E-10	2.23E-10	2.23E-10	2.24E-10	2.24E-10	2.26E-10
U	1.39E-04	4.26E-07	4.27E-07	1.83E-02	2.15E-03	1.00E-16
Zr	6.94E-10	6.68E-10	6.67E-10	6.72E-10	6.70E-10	6.78E-10

Total U losses (moles) for any of the runs can be estimated for any specific time increment from the U level solution composition in the tables ($U_{solution}$) via:

Moles U lost = $U_{solution}$ (mol/l) × time elapsed (y) × 1000 l/m^3 × water percolation rate (m^3/y)

The means for calculating the remaining mass of WP components is outlined in Attachment III.

Table 5-12. Elemental Composition of Corrosion Products (mole%) and Density for Case 4 (s01a1133)

Element \ Time (y)	242	10362	30411	57629
O	6.01E+01	6.00E+01	5.99E+01	5.98E+01
Al	3.13E-03	1.14E-01	2.53E-01	3.70E-01
B	6.42E-18	1.98E-19	2.98E-19	1.03E-14
Ba	3.27E-05	1.02E-03	2.25E-03	3.31E-03
Ca	0.00E+00	3.73E-02	8.05E-02	1.40E-01
Cl	0.00E+00	1.48E-19	0.00E+00	0.00E+00
Cr	0.00E+00	1.41E-03	3.11E-03	0.00E+00
Cu	0.00E+00	2.00E-03	4.62E-03	7.45E-03
F	0.00E+00	2.10E-03	4.23E-03	5.57E-03
Fe	3.92E+01	3.63E+01	3.28E+01	2.99E+01
H	2.35E-02	7.13E-01	1.58E+00	2.43E+00
C	0.00E+00	0.00E+00	0.00E+00	7.75E-03
P	3.46E-04	6.31E-03	1.27E-02	1.67E-02
K	0.00E+00	7.81E-03	1.73E-02	3.42E-02
Li	0.00E+00	0.00E+00	1.49E-19	0.00E+00
Mg	0.00E+00	2.29E-02	5.08E-02	8.55E-02
Mn	4.18E-01	4.90E-01	5.80E-01	6.33E-01
Na	0.00E+00	6.90E-03	1.53E-02	3.28E-02
Ni	0.00E+00	4.81E-01	1.08E+00	1.43E+00
Pb	1.20E-05	3.89E-04	8.61E-04	1.26E-03
Pu	0.00E+00	7.99E-05	1.80E-04	2.65E-04
S	3.27E-05	0.00E+00	0.00E+00	0.00E+00
Si	2.69E-01	1.70E+00	3.49E+00	4.98E+00
Ti	5.45E-04	1.65E-02	3.65E-02	5.35E-02
U	5.07E-04	1.06E-02	2.32E-02	3.39E-02
Zr	1.11E-03	7.87E-04	5.92E-04	4.57E-04
Total	100%	100%	100%	100%
Total (kg)	7168	9883	12728	15996
Density (g/cm^3)	5.26	5.10	4.91	4.74

Tables 5-12 and 5-13 outline reaction under conditions of average steel corrosion, low HLW glass corrosion, high SNF corrosion, and high flow rates (0.15 m^3/y) – run s01a1133. High SNF degradation rates by themselves should lead to high U and Pu levels (in solution and in alteration phases), but high flushing rates tend to prevent accumulation. Significantly less hematite, clays, and oxides are predicted to form in run s01a1133 relative to other runs. The net loss of B, U, and Pu from the WP under these conditions is predicted to be relatively small.

Table 5-13. Solution Composition (mol/kg) in Selected Years for Case 4 (s01a1133)

Time (y) / pH / Element	242	10362	30411	57629
pH	3.42	6.82	6.82	8.29
Al	5.55E-05	2.77E-15	2.77E-15	7.26E-16
B	8.37E-04	8.19E-04	8.19E-04	8.19E-04
Ba	1.65E-07	1.52E-07	1.52E-07	2.35E-09
Ca	3.80E-04	2.96E-04	2.96E-04	1.62E-04
Cl	2.10E-04	2.10E-04	2.10E-04	2.10E-04
Cr	2.35E-03	2.15E-03	2.15E-03	4.32E-06
Cu	6.52E-06	2.15E-06	2.15E-06	3.27E-07
F	1.20E-04	1.16E-04	1.16E-04	1.18E-04
Fe	2.33E-07	1.54E-12	1.54E-12	1.21E-12
C	3.39E-05	1.46E-04	1.46E-04	3.30E-03
P	1.56E-03	8.94E-08	8.94E-08	3.05E-09
K	3.37E-04	3.21E-04	3.21E-04	2.95E-04
Li	5.84E-04	5.85E-04	5.85E-04	5.85E-04
Mg	1.76E-04	1.28E-04	1.28E-04	3.93E-05
Mn	5.94E-07	7.63E-14	7.63E-14	2.18E-16
Mo	3.62E-05	3.63E-05	3.63E-05	1.00E-16
N	1.85E-04	1.85E-04	1.85E-04	1.42E-04
Na	3.01E-03	3.00E-03	3.00E-03	3.01E-03
Ni	1.06E-03	3.54E-05	3.54E-05	3.88E-08
Np	1.09E-08	1.09E-08	1.09E-08	1.09E-08
Pb	9.22E-08	2.50E-10	2.50E-10	1.44E-09
Pu	1.69E-07	1.07E-12	1.07E-12	1.05E-12
S	1.71E-03	2.08E-04	2.08E-04	2.03E-04
Si	1.87E-04	1.87E-04	1.87E-04	1.92E-04
Ti	2.26E-10	2.26E-10	2.26E-10	2.26E-10
U	2.06E-05	6.55E-09	6.55E-09	1.89E-07
Zr	6.80E-10	6.78E-10	6.78E-10	6.78E-10

Table 5-14. Elemental Composition of Corrosion Products (mole%) and Density for Case 10 (s01a1222)

Element \ Time (y)	11654	31080	43817	61151
O	5.93E+01	5.95E+01	5.96E+01	5.96E+01
Al	1.43E+00	1.36E+00	1.31E+00	1.28E+00
B	1.51E-01	0.00E+00	0.00E+00	9.07E-20
Ba	1.36E-02	1.30E-02	1.25E-02	1.22E-02
Ca	2.78E-01	1.76E-01	1.40E-01	1.42E-01
Cl	4.92E-18	8.59E-20	1.36E-16	8.72E-04
Cr	4.85E-03	1.76E-02	1.70E-02	1.11E-02
Cu	3.86E-02	3.69E-02	3.22E-02	2.81E-02
F	5.45E-03	6.16E-03	4.48E-03	4.05E-03
Fe	1.55E+01	1.71E+01	1.80E+01	1.84E+01
H	6.92E+00	6.88E+00	6.63E+00	6.50E+00
C	3.02E-01	5.08E-14	4.25E-14	6.51E-04
P	1.64E-02	1.85E-02	1.92E-02	1.48E-02
K	6.96E-01	3.26E-01	2.27E-01	2.00E-01
Mg	5.60E-01	3.98E-01	2.86E-01	2.74E-01
Mn	6.37E-01	6.79E-01	6.98E-01	7.07E-01
Na	6.28E-01	6.18E-03	1.84E-02	3.89E-02
Ni	4.10E-01	7.15E-01	7.54E-01	7.18E-01
Pb	4.85E-03	4.64E-03	4.47E-03	4.36E-03
Pu	3.53E-05	3.38E-05	3.22E-05	0.00E+00
S	2.32E-16	3.63E-17	8.18E-14	4.12E-04
Si	1.30E+01	1.25E+01	1.21E+01	1.18E+01
Ti	2.06E-01	1.97E-01	1.89E-01	1.85E-01
U	0.00E+00	0.00E+00	1.16E-25	0.00E+00
Zr	2.86E-04	2.74E-04	2.63E-04	2.57E-04
Total	100%	100%	100%	100%
Total (kg)	20777	22267	23410	24130
Density (g/cm^3)	3.67	3.83	3.89	3.92

Tables 5-14 and 5-15 outline the results of run s01a1222. Input conditions were average steel corrosion rates, high HLW glass corrosion, average SNF corrosion, and average water flux (0.015 m^3/y). High HLW glass corrosion causes high pH and, consequently, high U (and Pu) leach rates. Accumulation of hematite is relatively inhibited while the accumulation of smectites is pronounced (see Figures 5-1 and 5-2).

Table 5-15. Solution Composition (mol/kg) in Selected Years for Case 10 (s01a1222)

Time (y) / pH / Element	1182.8	11654	31080	43817	61151
pH	10.05	8.70	7.52	5.78	6.90
Al	7.41E-10	7.39E-08	8.36E-09	2.61E-05	2.28E-09
B	2.22E-01	2.31E-01	1.24E-05	1.24E-05	1.24E-05
Ba	2.02E-11	8.50E-10	3.74E-08	1.68E-07	1.31E-06
Ca	4.30E-06	9.98E-05	6.60E-03	1.71E-04	2.26E-05
Cl	2.56E-02	2.01E-04	2.01E-04	2.01E-04	2.01E-04
Cr	3.32E-02	2.15E-02	2.15E-02	2.15E-02	1.83E-04
Cu	4.97E-04	5.73E-07	4.87E-07	2.68E-04	6.05E-06
F	1.18E-02	8.52E-05	8.51E-05	2.75E-04	4.16E-11
Fe	4.11E-12	1.32E-12	1.24E-12	6.21E-12	1.47E-12
C	1.81E+00	1.13E-02	7.26E-04	4.50E-05	1.62E-04
P	2.47E-04	1.28E-07	5.87E-10	3.36E-05	5.46E-04
K	2.09E-01	5.37E-03	1.07E-02	1.51E-03	4.95E-04
Li	1.53E+00	6.92E-06	6.92E-06	6.92E-06	6.92E-06
Mg	2.85E-06	1.18E-04	9.36E-03	5.65E-04	6.93E-05
Mn	8.88E-15	3.26E-16	5.23E-15	1.34E-11	6.97E-14
Mo	3.46E-04	3.63E-04	3.63E-04	3.63E-04	1.00E-16
N	5.58E-04	5.72E-04	5.72E-04	5.72E-04	1.42E-04
Na	1.72E+00	1.18E-01	2.11E-03	1.28E-03	1.02E-03
Ni	7.85E-11	3.08E-08	5.48E-06	1.11E-02	4.17E-05
Np	3.13E-05	1.06E-16	1.00E-16	1.00E-16	1.00E-16
Pb	1.62E-12	8.84E-11	6.32E-11	2.82E-10	2.94E-11
Pu	4.84E-04	4.62E-10	4.34E-13	2.50E-08	3.95E-10
S	3.24E-02	2.48E-04	2.48E-04	2.48E-04	1.28E-04
Si	1.91E-03	4.07E-05	3.63E-05	5.97E-05	5.12E-05
Ti	1.56E-10	2.25E-10	2.26E-10	2.26E-10	2.26E-10
U	6.14E-02	1.46E-12	1.00E-16	1.00E-16	1.00E-16
Zr	4.88E-10	6.74E-10	6.77E-10	6.78E-10	6.78E-10

Tables 5-16 and 5-17 outline the results from run s01a2233 wherein initial conditions entailed high steel corrosion, high HLW glass corrosion, high SNF corrosion, and high flushing (0.15 m^3/y). Although the first should favor the formation of an acidic effluent, the second would favor the opposite, and the fourth condition would tend to work against both and instead maintain a baseline, near-neutral pH. The net effect is seen to be relatively constant pH, after an initial alkaline pulse. The early pulse is enough to effectively flush all of the U and most of the Pu from the system though. The otherwise near-neutral conditions favor maximal accumulation of hematite and smectites.

Table 5-16. Elemental Composition of Corrosion Products (mole%) and Density for Case 19 (s01a2233)

Element \ Time (y)	4382	10136	30460	62561
O	5.96E+01	5.96E+01	5.97E+01	5.97E+01
Al	1.31E+00	1.28E+00	1.26E+00	1.24E+00
B	0.00E+00	0.00E+00	0.00E+00	0.00E+00
Ba	1.25E-02	1.21E-02	1.20E-02	1.18E-02
Ca	1.36E-01	1.56E-01	2.26E-01	2.86E-01
Cl	1.34E-16	8.70E-04	8.60E-04	3.13E-20
Cr	1.69E-02	4.68E-31	4.65E-30	1.14E-30
Cu	3.38E-02	2.96E-02	2.92E-02	2.85E-02
F	5.19E-03	4.37E-03	4.45E-03	5.42E-03
Fe	1.80E+01	1.84E+01	1.82E+01	1.79E+01
H	6.62E+00	6.50E+00	6.56E+00	6.66E+00
C	0.00E+00	1.21E-02	1.20E-02	1.60E-02
P	1.94E-02	1.57E-02	1.59E-02	1.63E-02
K	2.47E-01	1.80E-01	8.38E-02	4.18E-02
Mg	2.83E-01	2.67E-01	2.53E-01	2.31E-01
Mn	6.97E-01	7.05E-01	6.97E-01	6.85E-01
Na	1.49E-02	5.06E-02	5.10E-02	4.91E-02
Ni	8.01E-01	7.63E-01	7.55E-01	7.41E-01
Pb	4.46E-03	4.35E-03	4.30E-03	4.22E-03
Pu	6.76E-04	4.11E-04	4.06E-04	3.99E-04
S	8.07E-14	1.59E-18	2.99E-17	8.42E-18
Si	1.21E+01	1.19E+01	1.20E+01	1.23E+01
Ti	1.89E-01	1.84E-01	1.82E-01	1.79E-01
U	1.14E-25	0.00E+00	0.00E+00	0.00E+00
Zr	2.63E-04	2.56E-04	2.53E-04	2.48E-04
Total	100%	100%	100%	100%
Total (kg)	23453	24199	24382	24695
Density (g/cm^3)	3.90	3.92	3.91	3.88

Table 5-17. Solution Composition (mol/kg) in Selected Years for Case 19 (s01a2233)

Time (y) / pH / Element	204.15	4381.7	10136	30460	62561
pH	9.59	5.78	8.08	8.08	8.08
Al	1.80E-08	2.86E-05	2.48E-08	2.48E-08	2.47E-08
B	2.07E-01	1.24E-05	1.24E-05	1.24E-05	1.24E-05
Ba	4.22E-11	1.68E-07	5.78E-09	5.83E-09	5.88E-09
Ca	8.20E-06	1.68E-04	5.23E-05	1.38E-04	2.36E-04
Cl	2.86E-03	2.01E-04	2.01E-04	2.01E-04	2.01E-04
Cr	2.30E-02	2.15E-02	1.00E-16	1.00E-16	1.00E-16
Cu	2.71E-05	2.65E-04	3.26E-07	3.26E-07	3.26E-07
F	1.23E-03	2.90E-04	1.14E-04	1.14E-04	1.14E-04
Fe	2.61E-12	6.18E-12	1.19E-12	1.19E-12	1.19E-12
C	1.70E-01	4.51E-05	2.03E-03	2.03E-03	2.02E-03
P	1.11E-05	3.37E-05	2.83E-08	5.82E-09	2.46E-09
K	2.28E-02	1.74E-03	6.24E-04	3.10E-04	1.59E-04
Li	1.67E-01	6.92E-06	6.92E-06	6.92E-06	6.92E-06
Mg	6.58E-06	6.21E-04	1.23E-04	1.25E-04	1.11E-04
Mn	2.28E-15	1.33E-11	3.12E-16	3.14E-16	3.16E-16
Mo	3.61E-04	3.63E-04	1.00E-16	1.00E-16	1.00E-16
N	5.76E-04	5.72E-04	1.42E-04	1.42E-04	1.42E-04
Na	2.65E-01	1.10E-03	1.87E-03	2.01E-03	1.99E-03
Ni	7.51E-10	1.10E-02	2.11E-07	2.13E-07	2.16E-07
Np	3.26E-06	1.00E-16	1.00E-16	1.00E-16	1.00E-16
Pb	1.46E-11	2.81E-10	1.18E-09	3.12E-09	3.61E-09
Pu	1.49E-05	2.55E-08	4.92E-13	4.92E-13	4.91E-13
S	3.79E-03	2.48E-04	1.92E-04	1.92E-04	1.92E-04
Si	1.47E-04	5.94E-05	3.94E-05	3.92E-05	3.90E-05
Ti	2.19E-10	2.26E-10	2.26E-10	2.26E-10	2.26E-10
U	6.43E-03	1.00E-16	1.00E-16	1.00E-16	1.00E-16
Zr	6.56E-10	6.78E-10	6.78E-10	6.78E-10	6.78E-10

Tables 5-18 and 5-19 describe the results of run s04a2204/s04b2022, the multi-stage calculation involving initial high steel and HLW glass corrosion, no SNF corrosion, and an extremely high flushing rate (0.5 m^3/y), followed by high steel corrosion, no HLW glass corrosion, average SNF corrosion, and average water flux (0.015 m^3/y). The net result of the boundary conditions is an initial sub-neutral pH period followed by a much longer period in which pH ~8 (Table 5-19). The early stage results in the formation of hematite, clays, and PuO_2. A substantial fraction of the latter (~30%) is ultimately flushed away under the ensuing alkaline conditions. Uranium is retained as a corrosion product for only a relatively brief period of time. Complete U removal is the ultimate outcome.

Table 5-18. Elemental Composition of Corrosion Products (mole%) and Density for Case 21 (s03a2204/s03b2022)

Time (y) / Element	4398	10001	32804	102490	633840
O	5.96E+01	5.97E+01	5.97E+01	5.97E+01	5.97E+01
Al	1.35E+00	1.28E+00	1.27E+00	1.27E+00	1.23E+00
B	0.00E+00	0.00E+00	4.10E-19	0.00E+00	0.00E+00
Ba	1.29E-02	1.21E-02	1.21E-02	1.21E-02	1.17E-02
Ca	1.91E-01	1.78E-01	1.87E-01	2.08E-01	2.98E-01
Cl	3.04E-16	1.25E-17	2.69E-04	8.64E-04	0.00E+00
Cr	1.75E-02	1.65E-02	2.99E-03	2.04E-31	3.46E-31
Cu	3.68E-02	2.71E-02	2.70E-02	2.69E-02	2.59E-02
F	6.35E-03	3.31E-03	5.10E-03	4.53E-03	5.56E-03
Fe	1.72E+01	1.84E+01	1.83E+01	1.83E+01	1.77E+01
Gd	3.33E-25	3.38E-26	0.00E+00	2.21E-29	2.82E-29
H	6.93E+00	6.55E+00	6.56E+00	6.58E+00	6.74E+00
C	2.94E-14	2.03E-14	1.21E-02	1.21E-02	1.59E-02
P	1.90E-02	2.02E-02	1.61E-02	1.62E-02	1.67E-02
K	1.18E-01	1.05E-01	9.62E-02	7.36E-02	3.52E-02
Li	1.43E-17	8.03E-19	0.00E+00	3.50E-21	0.00E+00
Mg	3.21E-01	2.95E-01	2.92E-01	2.79E-01	2.31E-01
Mn	6.82E-01	7.04E-01	7.04E-01	7.01E-01	6.81E-01
Mo	0.00E+00	0.00E+00	8.76E-32	2.18E-31	0.00E+00
N	3.00E-15	1.37E-16	0.00E+00	0.00E+00	6.21E-20
Na	2.30E-02	2.40E-02	4.22E-02	4.77E-02	4.95E-02
Ni	7.03E-01	6.57E-01	6.55E-01	6.52E-01	6.33E-01
Np	9.38E-25	5.06E-26	0.00E+00	3.20E-29	4.10E-29
Pb	4.61E-03	4.34E-03	4.34E-03	4.32E-03	4.19E-03
Pu	9.58E-04	9.02E-04	6.15E-04	6.13E-04	5.95E-04
S	1.67E-13	8.82E-15	0.00E+00	1.53E-18	2.02E-18
Si	1.26E+01	1.19E+01	1.19E+01	1.20E+01	1.24E+01
Tc	0.00E+00	0.00E+00	1.17E-31	2.18E-32	0.00E+00
Ti	1.95E-01	1.84E-01	1.84E-01	1.83E-01	1.78E-01
U	4.71E-25	7.93E-05	8.12E-05	3.72E-05	0.00E+00
Zr	1.97E-25	2.34E-04	2.56E-04	2.55E-04	2.47E-04
Total	100%	100%	100%	100%	100%
Total (kg)	22378	24166	24181	24242	24765
Density (g/cm^3)	3.84	3.92	3.91	3.91	3.87

Table 5-19. Solution Composition (mol/kg) in Selected Years for Case 21 (s03a2204/s03b2022)

Time (y) / Element \ pH	4398	10001	32804	102490	633840
	6.06	6.06	8.08	8.08	8.08
Al	8.54E-07	3.53E-09	2.47E-08	2.47E-08	2.47E-08
B	1.24E-05	1.24E-05	1.24E-05	1.24E-05	1.24E-05
Ba	1.93E-07	2.46E-07	5.96E-09	5.85E-09	5.89E-09
Ca	1.51E-04	8.11E-05	1.20E-04	1.25E-04	2.53E-04
Cl	2.01E-04	2.01E-04	1.78E-04	2.01E-04	2.01E-04
Cr	5.08E-03	3.66E-03	1.15E-04	1.00E-16	1.00E-16
Cu	5.64E-05	5.57E-05	3.26E-07	3.26E-07	3.26E-07
F	1.10E-04	4.50E-06	1.37E-04	1.14E-04	1.14E-04
Fe	3.53E-12	3.53E-12	1.19E-12	1.19E-12	1.19E-12
C	5.39E-05	5.38E-05	2.03E-03	2.02E-03	2.02E-03
P	7.89E-06	5.98E-05	7.51E-09	6.97E-09	2.20E-09
K	5.70E-04	3.68E-04	4.19E-04	2.86E-04	1.33E-04
Li	6.92E-06	6.92E-06	6.92E-06	6.92E-06	6.92E-06
Mg	3.57E-04	1.57E-04	2.31E-04	1.68E-04	1.09E-04
Mn	2.78E-12	2.68E-12	3.18E-16	3.15E-16	3.16E-16
N	2.41E-04	2.21E-04	1.42E-04	1.42E-04	1.42E-04
Na	1.18E-03	8.92E-04	1.95E-03	1.97E-03	1.99E-03
Ni	2.34E-03	2.20E-03	2.19E-07	2.15E-07	2.16E-07
Pb	3.20E-10	4.07E-10	2.88E-09	2.83E-09	3.62E-09
Pu	4.20E-11	7.72E-08	4.95E-13	4.92E-13	4.91E-13
S	2.05E-04	2.02E-04	1.92E-04	1.92E-04	1.92E-04
Si	5.73E-05	5.92E-05	3.87E-05	3.90E-05	3.90E-05
Ti	2.26E-10	2.26E-10	2.26E-10	2.26E-10	2.26E-10
U	1.00E-16	2.34E-07	4.21E-07	4.09E-07	1.00E-16
Zr	1.00E-16	6.78E-10	6.78E-10	6.78E-10	6.78E-10

Tables 5-20 and 5-21 describe the results of run s04a2204/s04b2022, a multi-stage run identical to s03a2204/s03b2022 except hematite was suppressed and goethite was allowed to form instead. The results are qualitatively similar with two notable exceptions. The initial pH is somewhat lower, and the amount of Pu retained in the alteration phases is less. Roughly 3/4 of the initial Pu is ultimately flushed away. U removal is similar to the hematite case – removal is total. The absolute mass of iron oxide (with smectite) formed in each case is high.

Table 5-20. Elemental Composition of Corrosion Products (mole%) and Density for Case 22 (s04a2204/s04b2022)

Element \ Time (y)	3999	5332	10025	34072	103760	633820
O	5.65E+01	5.62E+01	5.60E+01	5.60E+01	5.60E+01	5.63E+01
Al	1.21E+00	1.13E+00	1.10E+00	1.10E+00	1.09E+00	1.07E+00
B	0.00E+00	1.14E-19	0.00E+00	2.99E-17	1.40E-17	0.00E+00
Ba	1.15E-02	1.08E-02	1.05E-02	1.04E-02	1.04E-02	1.02E-02
Ca	2.03E-01	1.84E-01	1.80E-01	1.86E-01	2.01E-01	2.68E-01
Cl	4.23E-16	0.00E+00	1.72E-07	1.67E-04	7.39E-04	2.70E-20
Cr	1.56E-02	1.46E-02	1.41E-02	2.87E-03	0.00E+00	1.78E-31
Cu	3.23E-02	1.81E-02	1.58E-02	1.57E-02	1.56E-02	1.51E-02
F	5.36E-03	1.69E-03	1.65E-03	3.44E-03	2.90E-03	3.85E-03
Fe	1.50E+01	1.56E+01	1.58E+01	1.58E+01	1.58E+01	1.55E+01
H	1.40E+01	1.46E+01	1.49E+01	1.49E+01	1.49E+01	1.45E+01
C	3.25E-14	0.00E+00	0.00E+00	1.05E-02	1.04E-02	1.39E-02
P	1.61E-02	1.68E-02	1.52E-02	1.08E-02	1.09E-02	1.16E-02
K	1.08E-01	9.81E-02	9.28E-02	8.55E-02	6.61E-02	3.21E-02
Mg	2.64E-01	2.41E-01	2.33E-01	2.31E-01	2.24E-01	1.99E-01
Mn	5.99E-01	6.03E-01	6.07E-01	6.07E-01	6.05E-01	5.93E-01
Mo	7.62E-32	4.57E-19	0.00E+00	8.81E-32	0.00E+00	0.00E+00
Na	2.04E-02	1.65E-02	2.15E-02	3.86E-02	4.25E-02	4.48E-02
Ni	5.89E-01	5.53E-01	5.44E-01	5.42E-01	5.41E-01	5.30E-01
Pb	4.12E-03	3.86E-03	3.74E-03	3.74E-03	3.73E-03	3.65E-03
Pu	8.54E-04	8.00E-04	5.05E-04	1.97E-04	1.96E-04	1.92E-04
S	1.79E-13	1.32E-04	7.04E-16	0.00E+00	0.00E+00	1.69E-18
Si	1.12E+01	1.05E+01	1.03E+01	1.03E+01	1.03E+01	1.08E+01
Tc	2.08E-32	1.04E-31	1.01E-31	0.00E+00	0.00E+00	0.00E+00
Ti	1.74E-01	1.63E-01	1.59E-01	1.58E-01	1.58E-01	1.55E-01
U	5.51E-25	1.57E-05	6.91E-05	6.39E-05	1.28E-05	0.00E+00
Zr	2.05E-25	4.95E-05	2.17E-04	2.20E-04	2.20E-04	2.15E-04
Total	100%	100%	100%	100%	100%	100%
Total (kg)	22792	24334	25085	25100	25157	25647
Density (g/cm^3)	3.64	3.68	3.69	3.69	3.69	3.66

Table 5-21. Solution Composition (mol/kg) in Selected Years for Case 22 (s04a2204/s04b2022)

Time (y) / pH / Element	3999 / 5.81	5332 / 5.16	8381 / 5.35	10025 / 6.07	34072 / 8.08	103760 / 8.08	633820 / 8.08
Al	4.10E-06	5.24E-04	3.64E-05	2.16E-09	2.46E-08	2.47E-08	2.47E-08
B	1.24E-05	1.45E-04	1.24E-05	1.24E-05	1.24E-05	1.24E-05	1.24E-05
Ba	2.96E-07	5.06E-07	3.75E-07	4.98E-07	6.02E-09	5.87E-09	5.90E-09
Ca	2.26E-04	2.65E-03	3.08E-04	1.07E-04	1.56E-04	1.59E-04	2.62E-04
Cl	2.01E-04	2.01E-04	2.01E-04	2.01E-04	1.85E-04	2.01E-04	2.01E-04
Cr	5.08E-03	2.09E-01	4.55E-02	1.35E-03	8.93E-05	1.00E-16	1.00E-16
Cu	1.71E-04	4.49E-03	3.92E-04	4.66E-05	3.26E-07	3.26E-07	3.26E-07
F	1.12E-04	1.40E-03	1.57E-04	4.32E-07	1.31E-04	1.14E-04	1.14E-04
Fe	1.63E-11	8.96E-11	5.90E-11	1.02E-11	3.60E-12	3.60E-12	3.60E-12
C	4.52E-05	3.37E-05	3.75E-05	5.38E-05	2.01E-03	2.02E-03	2.02E-03
P	1.22E-05	2.81E-05	5.86E-04	5.90E-05	4.81E-09	4.66E-09	2.08E-09
K	5.82E-04	1.58E-03	5.51E-04	3.63E-04	4.06E-04	2.87E-04	1.34E-04
Li	6.92E-06	6.92E-06	6.92E-06	6.92E-06	6.92E-06	6.92E-06	6.92E-06
Mg	2.95E-04	2.38E-03	3.01E-04	1.17E-04	1.73E-04	1.36E-04	9.83E-05
Mn	8.58E-12	4.57E-10	1.20E-10	2.23E-12	3.20E-16	3.15E-16	3.16E-16
Mo	1.00E-16	3.52E-03	3.63E-03	9.59E-05	1.00E-16	1.00E-16	1.00E-16
N	2.41E-04	4.33E-03	1.14E-03	1.68E-04	1.42E-04	1.42E-04	1.42E-04
Na	1.16E-03	2.67E-03	1.18E-03	8.94E-04	1.94E-03	1.96E-03	1.99E-03
Ni	1.93E-03	1.03E-01	2.71E-02	4.95E-04	4.83E-08	4.71E-08	4.73E-08
Pb	4.90E-10	8.96E-10	6.37E-10	8.23E-10	3.70E-09	3.60E-09	3.62E-09
Pu	1.91E-10	1.87E-07	9.39E-05	4.94E-08	4.90E-13	4.91E-13	4.91E-13
S	2.05E-04	1.71E-03	3.22E-04	1.95E-04	1.92E-04	1.92E-04	1.92E-04
Si	3.29E-05	3.52E-05	3.67E-05	3.22E-05	2.12E-05	2.14E-05	2.14E-05
Ti	2.26E-10	2.23E-10	2.26E-10	2.26E-10	2.26E-10	2.26E-10	2.26E-10
U	1.00E-16	9.14E-07	1.05E-06	3.82E-08	5.52E-07	5.51E-07	1.00E-16
Zr	1.00E-16	6.69E-10	6.76E-10	6.78E-10	6.78E-10	6.78E-10	6.78E-10

Tables 5-22 and 5-23 outline the results of the multi-stage run s02g1203/s02g1021 wherein, initially, steel corrosion was average while HLW glass corrosion and fluid fluxing were high, but no SNF corrosion occurred. The second stage entailed average steel corrosion, no HLW glass corrosion, moderate SNF corrosion, and minimal fluid fluxing (0.0015 m^3/y). Goethite was the iron oxide allowed to precipitate. Except for a dip in pH at 30,571 years, pH values were predicted to remain at ~8 throughout the run, allowing complete removal of U, but only minor removal of Pu. Average steel degradation rates result in relatively low accumulations of goethite (Figure 5-1). Initially high HLW glass corrosion coupled with average steel degradation resulted in a relatively high pH causing elevated smectite formation (Figure 5-2).

Table 5-22. Elemental Composition of Corrosion Products (mole%) and Density for Case 24 (s02g1203/s0sg1021)

Element \ Time (y)	2020	10070	30571	100180	152010
O	5.77E+01	5.75E+01	5.70E+01	5.67E+01	5.67E+01
Al	1.29E+00	1.24E+00	1.15E+00	1.04E+00	1.03E+00
B	0.00E+00	0.00E+00	9.03E-22	5.72E-21	0.00E+00
Ba	1.23E-02	1.18E-02	1.09E-02	9.80E-03	9.71E-03
Ca	6.49E-01	5.14E-01	3.20E-01	3.10E-01	3.11E-01
Cl	3.54E-17	1.57E-20	2.89E-20	0.00E+00	1.17E-19
Cr	3.23E-16	4.23E-03	1.48E-02	0.00E+00	3.67E-30
Cu	3.51E-02	3.39E-02	2.08E-02	1.20E-03	1.08E-03
F	5.27E-03	5.52E-03	5.87E-03	6.01E-03	6.11E-03
Fe	1.26E+01	1.33E+01	1.43E+01	1.49E+01	1.48E+01
H	1.23E+01	1.27E+01	1.34E+01	1.39E+01	1.38E+01
C	5.11E-01	2.60E-01	5.48E-15	1.33E-02	1.32E-02
P	1.58E-02	1.65E-02	1.76E-02	1.80E-02	1.83E-02
K	4.45E-02	2.75E-02	2.21E-02	3.08E-02	3.15E-02
Mg	4.29E-01	3.25E-01	2.24E-01	1.99E-01	1.95E-01
Mn	5.39E-01	5.49E-01	5.68E-01	5.73E-01	5.68E-01
Mo	0.00E+00	0.00E+00	2.89E-20	5.95E-32	0.00E+00
Na	4.51E-02	1.77E-02	4.72E-02	4.74E-02	4.61E-02
Ni	2.09E-01	3.25E-01	4.69E-01	4.96E-01	4.91E-01
Pb	4.38E-03	4.23E-03	3.90E-03	3.53E-03	3.50E-03
Pu	9.27E-04	8.95E-04	8.26E-04	7.47E-04	7.41E-04
S	1.19E-14	1.57E-20	0.00E+00	0.00E+00	2.75E-17
Si	1.34E+01	1.30E+01	1.22E+01	1.16E+01	1.18E+01
Ti	1.86E-01	1.79E-01	1.65E-01	1.50E-01	1.48E-01
U	0.00E+00	7.75E-05	5.97E-05	3.45E-31	0.00E+00
Zr	3.36E-26	2.50E-04	2.30E-04	2.08E-04	2.06E-04
Total	100%	100%	100%	100%	100%
Total (kg)	20893	21809	23878	26463	26679
Density (g/cm^3)	3.47	3.52	3.59	3.62	3.61

Table 5-23. Solution Composition (mol/kg) in Selected Years for Case 24 (s02g1203/s02g1021)

Time (y) / pH / Element	2020	10070	30571	62550	100180	152010
pH	8.13	7.72	5.88	8.08	8.09	8.10
Al	2.77E-08	1.18E-08	2.80E-06	2.46E-08	6.81E-19	6.74E-19
B	1.24E-05	1.24E-05	1.24E-05	1.24E-05	1.24E-05	1.24E-05
Ba	4.76E-09	4.03E-08	3.12E-07	5.91E-09	5.51E-09	5.45E-09
Ca	2.63E-04	2.32E-03	2.99E-04	2.79E-04	3.05E-04	3.18E-04
Cl	2.01E-04	2.01E-04	2.01E-04	2.01E-04	2.01E-04	2.01E-04
Cr	3.05E-05	3.87E-03	3.87E-03	2.38E-10	1.00E-16	1.00E-16
Cu	3.25E-07	3.74E-07	1.21E-04	3.26E-07	3.25E-07	3.25E-07
F	1.14E-04	1.09E-04	1.11E-04	1.14E-04	1.14E-04	1.14E-04
Fe	3.61E-12	3.63E-12	1.43E-11	3.60E-12	3.60E-12	3.60E-12
C	2.28E-03	9.78E-04	4.70E-05	2.02E-03	2.10E-03	2.11E-03
P	2.04E-09	4.17E-10	5.19E-06	1.87E-09	1.59E-09	1.48E-09
K	1.85E-04	2.92E-04	8.36E-05	1.08E-04	1.23E-04	1.28E-04
Li	6.92E-06	6.92E-06	6.92E-06	6.92E-06	6.92E-06	6.92E-06
Mg	2.35E-04	1.34E-03	1.05E-04	9.05E-05	9.07E-05	8.97E-05
Mn	2.81E-16	1.49E-15	6.08E-12	3.17E-16	3.04E-16	3.02E-16
Mo	1.00E-16	6.53E-05	6.53E-05	1.00E-16	1.00E-16	1.00E-16
N	1.42E-04	2.19E-04	2.19E-04	1.42E-04	1.42E-04	1.42E-04
Na	1.99E-03	1.99E-03	1.89E-03	1.99E-03	2.01E-03	1.99E-03
Ni	3.81E-08	3.17E-07	1.37E-03	4.74E-08	4.42E-08	4.37E-08
Pb	2.92E-09	1.46E-10	5.16E-10	3.63E-09	3.39E-09	3.35E-09
Pu	5.62E-13	3.74E-13	2.45E-11	4.91E-13	5.10E-13	5.13E-13
S	1.92E-04	2.02E-04	2.02E-04	1.92E-04	1.92E-04	1.92E-04
Si	2.08E-05	2.08E-05	3.32E-05	2.14E-05	1.90E-04	1.90E-04
Ti	2.26E-10	2.26E-10	2.26E-10	2.26E-10	2.26E-10	2.26E-10
U	1.00E-16	1.15E-07	5.98E-08	5.49E-07	1.00E-16	1.00E-16
Zr	1.00E-16	6.78E-10	6.78E-10	6.78E-10	6.78E-10	6.78E-10

Table 5-24 shows results from cases 28 and 21a and compares the total density of the corrosion products estimated under conditions when hematite was allowed to form and when hematite was suppressed and goethite was allowed to form. Note that very little difference is observed between the two end-members.

Table 5-24. Comparison of Elemental Composition of Corrosion Products (mole%) and Density for Case 28 (s04c2204) and Calculated from Case 21a (s03a2204)

Case	S04c2204 with Goethite (hematite suppressed)		Calculated from S03a2204 with Hematite for $Fe_2O_3+H_2O=2FeOOH$	
Time (y)	4398		4398	
Element	Mole%	Mass (kg)	Mole%	Mass (kg)
O	5.65E+01	9.47E+03	5.61E+01	9.57E+03
Al	1.19E+00	3.37E+02	1.17E+00	3.37E+02
B	0.00E+00	0.00E+00	0.00E+00	0.00E+00
Ba	1.13E-02	1.63E+01	1.11E-02	1.63E+01
Ca	2.03E-01	8.53E+01	1.65E-01	7.07E+01
Cl	8.45E-16	3.14E-13	1.74E-15	6.58E-13
Cr	1.54E-02	8.40E+00	1.51E-02	8.40E+00
Cu	2.86E-02	1.90E+01	3.18E-02	2.16E+01
F	5.32E-03	1.06E+00	5.49E-03	1.11E+00
Fe	1.51E+01	8.84E+03	1.48E+01	8.84E+03
Gd	7.21E-25	1.19E-21	1.90E-24	3.19E-21
H	1.41E+01	1.49E+02	1.50E+01	1.62E+02
C	9.10E-14	1.15E-11	3.20E-13	4.10E-11
P	1.60E-02	5.18E+00	1.65E-02	5.44E+00
K	9.94E-02	4.08E+01	1.02E-01	4.24E+01
Li	3.20E-17	2.33E-15	8.17E-17	6.05E-15
Mg	2.57E-01	6.55E+01	2.77E-01	7.20E+01
Mn	6.00E-01	3.46E+02	5.89E-01	3.46E+02
Mo	2.12E-31	2.13E-28	0.00E+00	0.00E+00
N	5.65E-15	8.29E-13	1.71E-14	2.56E-12
Na	3.13E-02	7.55E+00	1.99E-02	4.88E+00
Ni	5.85E-01	3.60E+02	6.07E-01	3.81E+02
Np	2.00E-24	4.98E-21	5.36E-24	1.36E-20
Pb	4.06E-03	8.82E+00	3.99E-03	8.82E+00
Pu	8.42E-04	2.11E+00	8.28E-04	2.11E+00
S	3.42E-13	1.15E-10	1.07E-12	3.66E-10
Si	1.11E+01	3.27E+03	1.09E+01	3.26E+03
Tc	0.00E+00	0.00E+00	0.00E+00	0.00E+00
Ti	1.72E-01	8.64E+01	1.69E-01	8.64E+01
U	1.17E-24	2.93E-21	2.69E-24	6.82E-21
Zr	4.16E-25	3.98E-22	1.13E-24	1.10E-21
Total	100%	23121	100%	23248
Density (g/cm^3)	3.65		3.65	

Recall that U is contained in both the Shippingport SNF and in the HLW glass, and that the isotopic ratios of the two sources differ. It is important for subsequent neutronics calculations that the relative contribution of the two be estimated over time. This estimate was done in part through runs 29 and 30 which had inputs identical to runs 1 and 10, except that the original U component in the HLW glass (~1.8%) was replaced with Ti in the input. This allows the U release from the SNF to be isolated. Comparison of the results of runs 29 and 30 (U in SNF) against the results of runs 1 and 10 (U in HLW glass and SNF) allows the relative U contribution from the HLW glass and SNF over time to be assessed. This comparison is made in Figures 5-3 and 5-4. In the first case – average steel corrosion, low HLW glass corrosion, low SNF corrosion, and low fluid flux (Figure 5-3) – the total U in the WP is primarily from the HLW glass, at least until ~ 500,000 years have elapsed. In the second case – average steel corrosion, high HLW glass corrosion, average SNF corrosion, and average flow (Figure 5-4) – the total U in the WP is primarily from the SNF, except over the first 500 years wherein the situation is reversed.

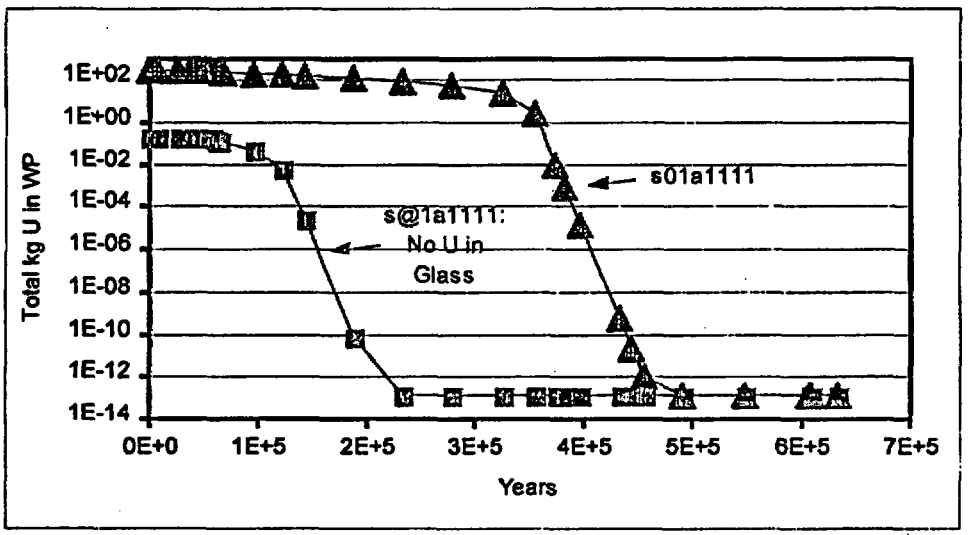

Figure 5-3. Predicted Total U Mass in WP for Runs s@1a1111 and s01a1111 (see text)

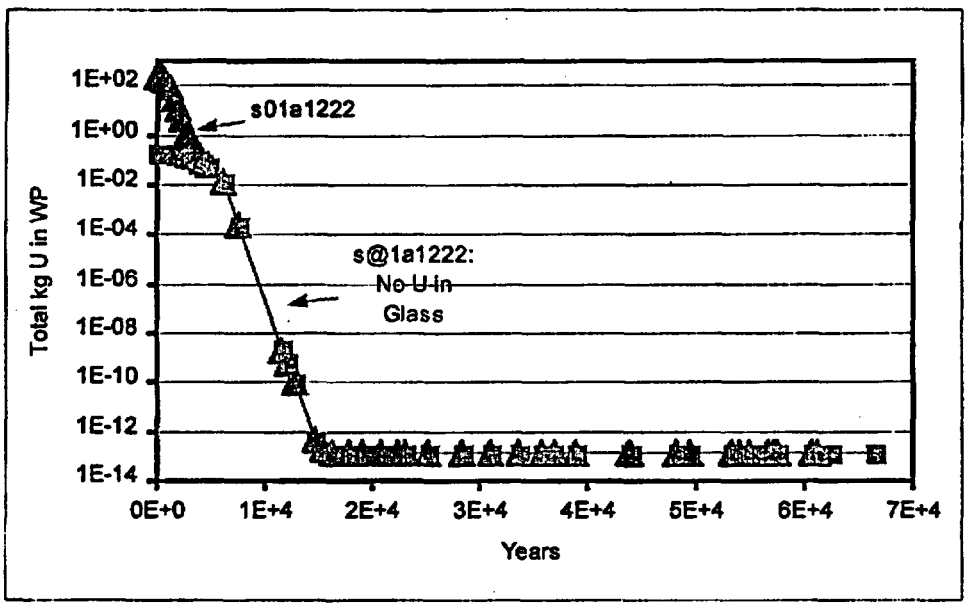

Figure 5-4. Predicted Total U Mass in WP for Runs s01a1222 and s@1a1222 (see text)

Runs 25-27 were done to test the effect of 100% SNF exposure on B, Pu, and U release from the WP. The effect was found to be minimal, except for case 27, wherein U loss was found to be decreased somewhat. The rest of the cases were run assuming that only 1% of the moles and surface area of the SNF wafers was exposed to degradation during the simulations, i.e., the moles and surface area values entered for the SNF reactant were actually multiplied by 0.01 before entry in the input files.

6. RESULTS

The results of this Calculation are based on a combination of qualified and unqualified technical information. Therefore, use of any unqualified technical information or result from the Calculation as input in documents supporting construction, fabrication, or procurement, or as part of a verified design to be released to another organization, is required to be identified and controlled in accordance with appropriate procedures.

A principle objective of this calculation was to assess the chemical characteristics that might lead to the retention of U, B, and Pu in a WP containing Shippingport SNF and HLW glass. Thirty EQ6 reaction path calculations were carried out to span the range of possible system behavior and to assess the specific and coupled effects of SNF degradation, steel corrosion, HLW glass degradation, and fluid influx rate on U and Pu mobilization. Fluids having a composition of J-13 well water were represented as steady-state reactants with WP components over time spans of up to 633,000 years. Corrosion product accumulation (primarily of iron oxide and smectite) and U, B, and Pu mobilization were examined as well.

In almost all cases, B mobilization was complete. U loss from the WP varied from 0.06% to 100% and was typically complete if greater-than-neutral pH (and attendant high alkalinity) existed for any appreciable amount of time. Immobilized U was represented as occurring due to the formation of the U-silicate soddyite. The relative contributions of U from HLW glass and U from SNF are predicted to vary. Under conditions of average steel corrosion, low HLW glass corrosion, low SNF corrosion, and low fluid flux, the total U in the WP is primarily from the HLW glass until ~500,000 years have elapsed. When average steel corrosion, high HLW glass corrosion, average SNF corrosion, and average flow are used as input, the total U in the WP is predicted to come primarily from the SNF, except over the first 500 years wherein the HLW glass contribution is greater.

Pu loss was typically much less than U, though WP accumulations were also quantitatively smaller than those observed for U. Pu accumulation was represented as being due to formation of PuO_2. Accessory corrosion products predicted to form included boehmite, pyrolusite, Ni_2SiO_4, and $NiFe_2O_4$.

Referring again to Table 5-9, the controls on B, U, and Pu release from the WP can be summarized as follows:

- B loss is complete except when HLW glass dissolution rates are low and water fluxes are high.
- U and Pu losses are greatest when HLW glass dissolution rates are high. At a given HLW glass dissolution rate, U loss varies inversely with the flux of water. Steel corrosion and SNF degradation are third-order controls over U and Pu release.

High HLW glass dissolution and low water fluxes favor alkalinity buildup and the formation of mobile actinide-carbonate complexes.

7. ATTACHMENTS

ATTACHMENT I. Sketch SK-0070 REV 02, 5-DHLW/DOE Spent Fuel Long Disposal Container (1 page)

ATTACHMENT II. Listing of Files on Electronic Media (CD) (4 pages)
(Reference 21 provides the electronic media.)

ATTACHMENT III. Calculating Remaining Mass (3 pages)

ATTACHMENT IV. Document Input Reference Sheets (10 pages)

8. REFERENCES

1 DOE (U.S. Department of Energy) 1999. *Shippingport PWR (HEU Oxide) Fuel Characteristics for Disposal Criticality Analysis.* DOE/SNF/REP-040, Revision 0. Washington, D.C.: U.S. Department of Energy. TIC: 243528.

2 CRWMS M&O 1998. *EQ6 Calculations for Chemical Degradation of Fast Flux Test Facility (FFTF) Waste Packages.* BBA000000-01717-0210-00028 REV 00. Las Vegas, Nevada: CRWMS M&O. ACC: MOL.19981229.0081.

3 CRWMS M&O 1998. "Disruptive Events." Chapter 10 of *Total System Performance Assessment-Viability Assessment (TSPA-VA) Analyses Technical Basis Document.* B00000000-01717-4301-00010 REV 00. Las Vegas, Nevada: CRWMS M&O. ACC: MOL.19980724.0399.

4 CRWMS M&O 1998. *Evaluation of Codisposal Viability for Aluminum-Clad DOE-Owned Spent Fuel: Phase II Degraded Codisposal Waste Package Internal Criticality.* BBA000000-01717-5705-00017 REV 01. Las Vegas, Nevada: CRWMS M&O. ACC: MOL.19981014.0038.

5 National Research Council 1995. *Technical Bases for Yucca Mountain Standards.* Washington, D.C.: National Academy Press. TIC: 217588.

6 Harrar, J.E.; Carley, J.F.; Isherwood, W.F.; and Raber, E. 1990. *Report of the Committee to Review the Use of J-13 Well Water in Nevada Nuclear Waste Storage Investigations.* UCID-21867. Livermore, California: Lawrence Livermore National Laboratory. ACC: NNA.19910131.0274.

7 DOE (U.S. Department of Energy) 1998. *Total System Performance Assessment.* Volume 3 of *Viability Assessment of a Repository at Yucca Mountain.* DOE/RW-0508. Washington, D.C.: U.S. Department of Energy, Office of Civilian Radioactive Waste Management. ACC: MOL.19981007.0030.

8 Yang, I.C.; Rattray, G.W.; and Yu, P. 1996. *Interpretation of Chemical and Isotopic Data from Boreholes in the Unsaturated Zone at Yucca Mountain, Nevada.* Water-Resources Investigations Report 96-4058. Denver, Colorado: U.S. Geological Survey. ACC: MOL.19980528.0216.

9 Weast, R.C. 1977. *CRC Handbook of Chemistry and Physics. 58th Edition.* Pages B-121 and F-210 . Cleveland, Ohio: CRC Press. TIC: 242376.

10 CRWMS M&O 1996. *Second Waste Package Probabilistic Criticality Analysis: Generation and Evaluation of Internal Criticality Configurations.* BBA000000-01717-2200-00005 REV 00. Las Vegas, Nevada: CRWMS M&O. ACC: MOL.19960924.0193.

11 Hillner, E.; Franklin, D.G.; and Smee, J.D. 1998. *The Corrosion of Zircaloy-Clad Fuel Assemblies in a Geologic Repository Environment.* WAPD-T-3173. West Mifflin, Pennsylvania: Bettis Atomic Power Laboratory. TIC: 237127.

12 CRWMS M&O 1999. *Addendum to: EQ6 Computer Program for Theoretical Manual, Users Guide, & Related Documentation.* Software Change Request (SCR) LSCR198. UCRL-MA-110662 PT IV. Las Vegas, Nevada: CRWMS M&O. ACC: MOL.19990305.0112.

13 CRWMS M&O 1998. *Software Qualification Report (SQR) Addendum to Existing LLNL Document UCRL-MA-110662 PT IV: Implementation of a Solid-Centered Flow-Through Mode for EQ6 Version 7.2b.* CSCI: UCRL-MA-110662 V 7.2B, SCR: LSR198, MI: 30084-M04-001 (Addendum Only). Las Vegas, Nevada: CRWMS M&O. ACC: MOL.19981214.0108.

14 CRWMS M&O 1998. *EQ6 Calculations for Chemical Degradation of Pu-Ceramic Waste Packages.* BBA000000-01717-0210-00018 REV 00. Las Vegas, Nevada: CRWMS M&O. ACC: MOL.19980918.0004.

15 CRWMS M&O 1998. *EQ3/6 Software Installation and Testing Report for Pentium Based Personal Computers (PCs).* CSCI: LLYMP9602100. Las Vegas, Nevada: CRWMS M&O. ACC: MOL.19980813.0191.

16 Wolery, T.J. 1992. *EQ3/6, A Software Package for Geochemical Modeling of Aqueous Systems. Package Overview and Installation Guide (Version 7.0).* UCRL-MA-110662 PT I. Livermore, California: Lawrence Livermore National Laboratory. TIC: 205087.

17 Daveler, S.A. and Wolery, T.J. 1992. *EQPT, A Data File Preprocessor for the EQ3/6 Software Package. User's Guide, and Related Documentation (Version 7.0).* UCRL-MA-110662 PT II. Livermore, California: Lawrence Livermore National Laboratory. TIC: 205240.

18 Wolery, T.J. 1992. *EQ3NR, A Computer Program for Geochemical Aqueous Speciation-Solubility Calculations. Theoretical Manual, User's Guide, and Related Documentation (Version 7.0).* UCRL-MA-110662 PT III. Livermore, California: Lawrence Livermore National Laboratory. TIC: 205154.

19 Wolery, T.J. and Daveler, S.A. 1992. *EQ6, A Computer Program for Reaction Path Modeling of Aqueous Geochemical Systems: Theoretical Manual, User's Guide, and*

Related Documentation (Version 7.0). UCRL-MA-110662 PT IV. Livermore, California: Lawrence Livermore National Laboratory. TIC: 205002.

20 Spahiu, K. and Bruno, J. 1995. *A Selected Thermodynamic Database for REE to be Used in HLNW Performance Assessment Exercises.* SKB Technical Report 95-35. Stockholm, Sweden: Swedish Nuclear Fuel and Waste Management Company. TIC: 225493.

21 CRWMS M&O 1999. *Electronic Media (CD): The Calculation Files for EQ6 Calculation for Chemical Degradation of Shippingport PWR Spent Nuclear Fuel Waste Packages, CAL-EDC-MD-000002 REV 00.* Las Vegas, Nevada: CRWMS M&O. ACC: MOL.19991118.0179.

22 CRWMS M&O 1998. *EQ6 Calculations for Chemical Degradation of PWR LEU and PWR MOX Spent Fuel Waste Packages.* BBA000000-01717-0210-00009 REV 00. Las Vegas, Nevada: CRWMS M&O. ACC: MOL.19980701.0483.

23 CRWMS M&O 1997. *Criticality Evaluation of Degraded Internal Configurations for the PWR AUCF WP Designs.* BBA000000-01717-0200-00056 REV 00. Las Vegas, Nevada: CRWMS M&O. ACC: MOL.19971231.0251.

24 CRWMS M&O 1999. *DOE SRS HLW Glass Chemical Composition.* BBA000000-01717-0210-00038 REV 00. Las Vegas, Nevada: CRWMS M&O. ACC: MOL.19990215.0397.

25 DOE (U.S. Department of Energy) 1992. *Characteristics of Potential Repository Wastes.* DOE/RW-0184-R1. Volume 1. Washington, D.C.: U.S. Department of Energy, Office of Civilian Radioactive Waste Management. ACC: HQO.19920827.0001.

26 CRWMS M&O 1995. *Total System Performance Assessment - 1995: An Evaluation of the Potential Yucca Mountain Repository.* B00000000-01717-2200-00136 REV 01. Las Vegas, Nevada: CRWMS M&O. ACC: MOL.19960724.0188.

27 CRWMS M&O 1998. "Near-Field Geochemical Environment." Chapter 4 of *Total System Performance Assessment-Viability Assessment (TSPA-VA) Analyses Technical Basis Document.* B00000000-01717-4301-00004 REV 01. Las Vegas, Nevada: CRWMS M&O. ACC: MOL.19981008.0004.

28 CRWMS M&O 1998. *Complete Draft VA UZ Abstraction/Test Document.* B00000000-01717-2200-00201. Las Vegas, Nevada: CRWMS M&O. ACC: MOL.19980428.0202.

29 CRWMS M&O 1996. *Status Report on Degraded Mode Criticality Analysis of Immobilized Plutonium Waste Forms in a Geologic Repository.* A00000000-01717-5705-00013 REV 00. Vienna, Virginia: CRWMS M&O. ACC: MOL.19970324.0023.

30 CRWMS M&O 1997. *Degraded Mode Criticality Analysis of Immobilized Plutonium Waste Forms in a Geologic Repository.* Predecisional Document. A00000000-01717-5705-00014 REV 01. Las Vegas, Nevada: CRWMS M&O. ACC: MOL.19980422.0911.

31 Roberts, W.L.; Rapp, G.R., Jr.; and Weber, J. 1974. *Encyclopedia of Minerals.* Pages 172, 240, 241, 413, 500, 689, and 690. New York, New York: Van Nostrand Reinhold. TIC: 238571.

32 CRWMS M&O 1996. *Material Compositions and Number Densities for Neutronics Calculations.* BBA000000-01717-0200-00002 REV 00. Las Vegas, Nevada: CRWMS M&O. ACC: MOL.19960624.0023.

33 Walker, F.W.; Parrington, J.R.; and Feiner, F. 1989. *Nuclides and Isotopes, Fourteenth Edition: Chart of the Nuclides.* San Jose, California: General Electric Company. TIC: 201637.

34 CRWMS M&O 1998. *Disposal Criticality Analysis Methodology Topical Report.* B00000000-01717-5705-00095 REV 00. Las Vegas, Nevada: CRWMS M&O. ACC: MOL.19980918.0005.

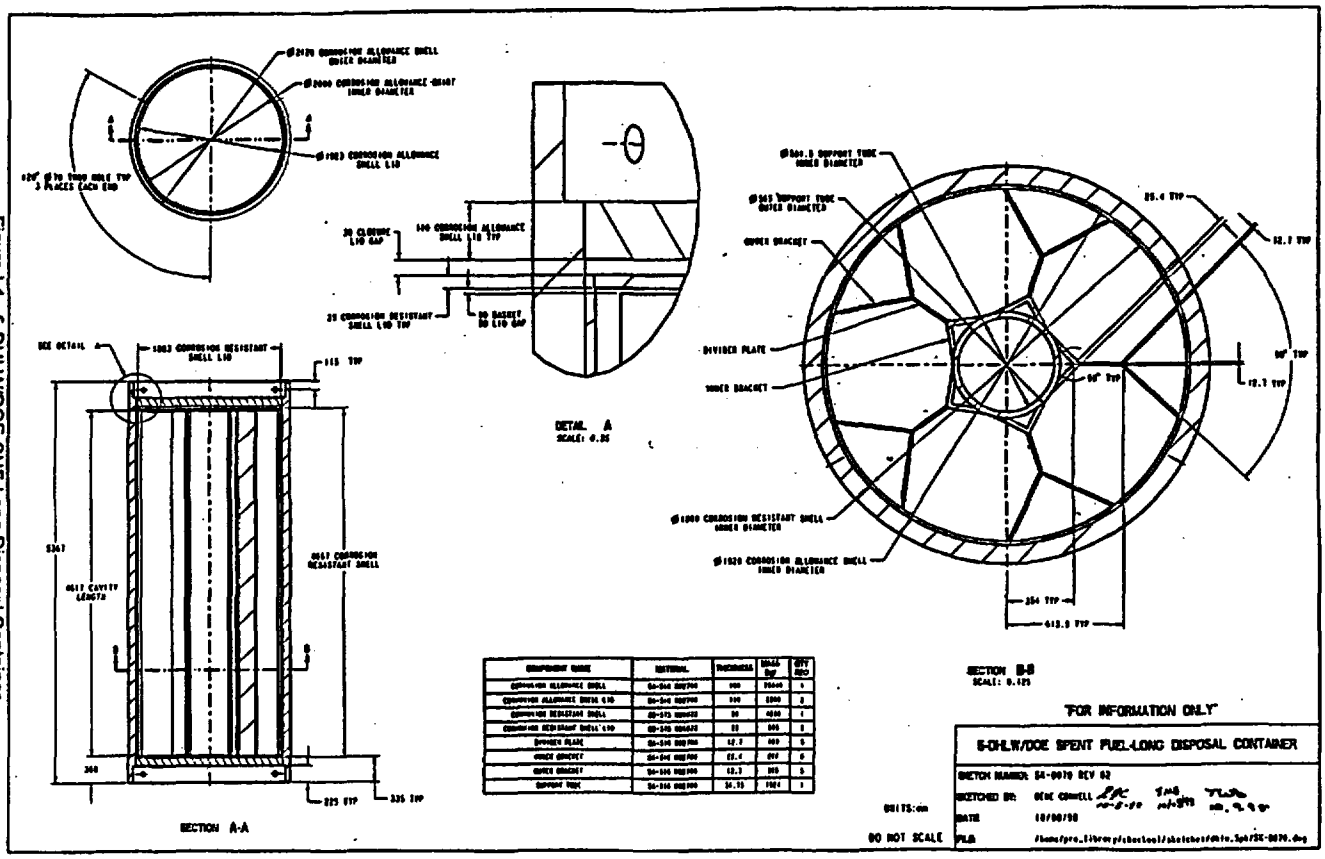

Figure I-1. 5-DHLW/DOE SNF-Long Disposal Container

ATTACHMENT II. LISTING OF FILES ON ELECTRONIC MEDIA (CD)

File Name	File Size (bytes)	Month	Day	Time
01shipBGdPuU.xls	393728	Sep	15	14:38
Attachments.doc	360960	Sep	15	11:46
DIRSspwr00b.doc	66048	Sep	15	11:45
Eq6.exe	1056469	Sep	15	14:40
Hematite_2_Goethite_HWS.xls	49152	May	13	11:35
RUNEQ6.EXE	392181	Sep	15	14:41
Sl1a1113.6i	44658	May	27	17:05
Sl1a1133.6i	44656	May	27	17:05
Sl2G2021.6i	44233	May	27	17:05
S01a1111.6i	44553	May	27	16:15
S01a1113.6i	44553	May	27	16:15
S01a1122.6i	44553	May	27	16:15
S01a1131.6i	44553	May	27	16:15
S01a1133.6i	44553	May	27	16:15
S01a1211.6i	44553	May	27	16:16
S01a1213.6i	44553	May	27	16:16
S01a1222.6i	44553	May	27	16:16
S01a1231.6i	44553	May	27	16:16
S01a1233.6i	44553	May	27	16:16
S01a2111.6i	44553	May	27	16:17
S01a2113.6i	44553	May	27	16:17
S01a2122.6i	44553	May	27	16:17
S01a2131.6i	44553	May	27	16:17
S01a2133.6i	44553	May	27	16:18
S01a2211.6i	44553	May	27	16:18
S01a2213.6i	44553	May	27	16:18
S01a2222.6i	44550	May	27	16:18
S01a2231.6i	44553	May	27	16:19
S01a2233.6i	44553	May	27	16:19
S01c1104.6i	36742	May	3	15:02
S01c1204.6i	36742	May	3	15:02
S01c2104.6i	36742	May	3	15:02
S01c2204.6i	36742	May	3	15:02
S01g1203.6i	36961	May	3	15:02
S01g2203.6i	36964	May	3	15:02
S01g2204.6i	36959	May	3	15:02
S02G2021.6l	44149	May	10	14:49
S02c2204.6i	36957	May	3	15:02
S02g1203.6i	37123	May	3	15:03
S02g2203.6i	37123	May	3	15:03
S02g2204.6i	37123	May	3	15:03
S03a2204.6i	37035	May	3	15:03
S04B2022.6l	44255	May	10	14:49
S04a2204.6i	37256	May	3	15:04
S04c2204.6l	37289	May	27	17:06
SHIP00.BAT	3673	Sep	15	14:41
ShipKL19sea.xls	423936	Aug	16	10:38
TableBUPu.doc	76800	May	13	11:35
complete.wav	12118	Jun	25	11:53
composition.doc	107008	May	13	11:35
copy_of_sl1a1113.elem_aqu.txt	77403	Jul	8	19:42
copy_of_sl1a1133.elem_aqu.txt	74739	Jul	8	19:42
copy_of_sl2g2021.elem_aqu.txt	100047	Jul	8	19:42
density_ship.xls	222720	May	13	11:35
eq6new.for 1	322426	Sep	15	14:41
eqlibnew.for	492613	Sep	15	14:41
fftf_short.xls	3695616	Sep	15	14:41
filesa.txt	0	Sep	15	15:15

File Name	File Size (bytes)	Month	Day	Time
j13evaporIIK3.xls	32256	Sep	15	14:41
no_U_glass	4096	Sep	10	16:22
sl1a1113.6o	8514554	May	27	17:05
sl1a1113.elem_aqu.txt	77403	May	27	17:05
sl1a1113.elem_min.txt	73234	May	27	17:05
sl1a1113.elem_tot.txt	73247	May	27	17:05
sl1a1133.6o	8296671	May	27	17:05
sl1a1133.6p	47999	May	27	17:05
sl1a1133.elem_aqu.txt	74739	May	27	17:05
sl1a1133.elem_min.txt	70714	May	27	17:05
sl1a1133.elem_tot.txt	70727	May	27	17:05
sl2g2021.6o	13069761	May	27	17:06
sl2g2021.6p	44799	May	27	17:06
sl2g2021.elem_aqu.txt	100047	May	27	17:06
sl2g2021.elem_min.txt	94654	May	27	17:06
sl2g2021.elem_tot.txt	94667	May	27	17:06
s01a1111.6o	4667339	May	27	16:15
s01a1111.elem_aqu.txt	45435	May	3	15:01
s01a1111.elem_min.txt	42994	May	3	15:01
s01a1111.elem_tot.txt	43007	May	3	15:01
s01a1113.6o	8437060	May	27	16:15
s01a1113.elem_aqu.txt	76515	May	3	15:01
s01a1113.elem_min.txt	72394	May	3	15:01
s01a1113.elem_tot.txt	72407	May	3	15:01
s01a1122.6o	9370228	May	27	16:15
s01a1122.elem_aqu.txt	82287	May	3	15:01
s01a1122.elem_min.txt	77854	May	3	15:02
s01a1122.elem_tot.txt	77867	May	3	15:02
s01a1131.6o	4689261	May	27	16:15
s01a1131.elem_aqu.txt	45435	May	3	15:02
s01a1131.elem_min.txt	42994	May	3	15:02
s01a1131.elem_tot.txt	43007	May	3	15:02
s01a1133.6o	8468483	May	27	16:16
s01a1133.elem_aqu.txt	76959	May	3	15:02
s01a1133.elem_min.txt	72814	May	3	15:02
s01a1133.elem_tot.txt	72827	May	3	15:02
s01a1211.6o	4595720	May	27	16:16
s01a1211.elem_aqu.txt	43659	May	3	15:02
s01a1211.elem_min.txt	41314	May	3	15:02
s01a1211.elem_tot.txt	41327	May	3	15:02
s01a1213.6o	8891329	May	27	16:16
s01a1213.elem_aqu.txt	76959	May	3	15:02
s01a1213.elem_min.txt	72814	May	3	15:02
s01a1213.elem_tot.txt	72827	May	3	15:02
s01a1222.6o	3601063	May	27	16:16
s01a1222.elem_aqu.txt	35667	May	3	15:02
s01a1222.elem_min.txt	33754	May	3	15:02
s01a1222.elem_tot.txt	33767	May	3	15:02
s01a1231.6o	4611903	May	27	16:16
s01a1231.elem_aqu.txt	43659	May	3	15:02
s01a1231.elem_min.txt	41314	May	3	15:02
s01a1231.elem_tot.txt	41327	May	3	15:02
s01a1233.6o	8028046	May	27	16:17
s01a1233.elem_aqu.txt	70743	May	3	15:02
s01a1233.elem_min.txt	66934	May	3	15:02
s01a1233.elem_tot.txt	66947	May	3	15:02
s01a2111.6o	4865034	May	27	16:17
s01a2111.elem_aqu.txt	48099	May	3	15:02
s01a2111.elem_min.txt	45514	May	3	15:02
s01a2111.elem_tot.txt	45527	May	3	15:02

File Name	File Size (bytes)	Month	Day	Time
s01a2113.6o	8435225	May	27	16:17
s01a2113.elem_aqu.txt	75627	May	3	15:02
s01a2113.elem_min.txt	71554	May	3	15:02
s01a2113.elem_tot.txt	71567	May	3	15:02
s01a2122.6o	9550093	May	27	16:17
s01a2122.elem_aqu.txt	84951	May	3	15:02
s01a2122.elem_min.txt	80374	May	3	15:02
s01a2122.elem_tot.txt	80387	May	3	15:02
s01a2131.6o	4902974	May	27	16:18
s01a2131.elem_aqu.txt	48543	May	3	15:02
s01a2131.elem_min.txt	45934	May	3	15:02
s01a2131.elem_tot.txt	45947	May	3	15:02
s01a2133.6o	8538448	May	27	16:18
s01a2133.elem_aqu.txt	76959	May	3	15:02
s01a2133.elem_min.txt	72814	May	3	15:02
s01a2133.elem_tot.txt	72827	May	3	15:02
s01a2211.6o	4436860	May	27	16:18
s01a2211.elem_aqu.txt	43215	May	3	15:02
s01a2211.elem_min.txt	40894	May	3	15:02
s01a2211.elem_tot.txt	40907	May	3	15:02
s01a2213.6o	9356574	May	27	16:18
s01a2213.elem_aqu.txt	82731	May	3	15:02
s01a2213.elem_min.txt	78274	May	3	15:02
s01a2213.elem_tot.txt	78287	May	3	15:02
s01a2222.6o	9351430	May	27	16:19
s01a2222.elem_aqu.txt	82731	May	3	15:02
s01a2222.elem_min.txt	78274	May	3	15:02
s01a2222.elem_tot.txt	78287	May	3	15:02
s01a2231.6o	6071668	May	27	16:19
s01a2231.elem_aqu.txt	49431	May	3	15:02
s01a2231.elem_min.txt	46774	May	3	15:02
s01a2231.elem_tot.txt	46787	May	3	15:02
s01a2233.6o	9066082	May	27	16:19
s01a2233.elem_aqu.txt	81843	May	3	15:02
s01a2233.elem_min.txt	77434	May	3	15:02
s01a2233.elem_tot.txt	77447	May	3	15:02
s01g1203.6o	3070328	May	3	15:02
s01g2203.6o	2475038	May	3	15:02
s02c2204.6o	5907605	May	3	15:02
s02g1021.6i	44159	May	3	15:02
s02g1021.6o	13135353	May	3	15:03
s02g1021.elem_aqu.txt	104931	May	3	15:03
s02g1021.elem_min.txt	99274	May	3	15:03
s02g1021.elem_tot.txt	99287	May	3	15:03
s02g1203.elem_aqu.txt	116919	May	3	15:03
s02g1203.elem_min.txt	110614	May	3	15:03
s02g1203.elem_tot.txt	110627	May	3	15:03
s02g2021.6i	44149	May	3	15:03
s02g2021.6o	12882692	May	3	15:03
s02g2021.elem_aqu.txt	99159	May	3	15:03
s02g2021.elem_min.txt	93814	May	3	15:03
s02g2021.elem_tot.txt	93827	May	3	15:03
s02g2203.elem_aqu.txt	117807	May	3	15:03
s02g2203.elem_min.txt	111454	May	3	15:03
s02g2203.elem_tot.txt	111467	May	3	15:03
s02g2204.6o	6080586	May	3	15:03
s03a2204.6o	3585722	May	3	15:03
s03a2204.elem_aqu.txt	33003	May	3	15:03
s03a2204.elem_min.txt	31234	May	3	15:03
s03a2204.elem_tot.txt	31247	May	3	15:03

File Name	File Size (bytes)	Month	Day	Time
s03b2022.6i	43764	May	3	15:03
s03b2022.6o	7193769	May	3	15:04
s03b2022.elem_aqu.txt	64083	May	3	15:04
s03b2022.elem_min.txt	60634	May	3	15:04
s03b2022.elem_tot.txt	60647	May	3	15:04
s04a2204.6o	3488141	May	3	15:04
s04a2204.elem_aqu.txt	32115	May	3	15:04
s04a2204.elem_min.txt	30394	May	3	15:04
s04a2204.elem_tot.txt	30407	May	3	15:04
s04b2022.6i	44255	May	3	15:04
s04b2022.elem_aqu.txt	66303	May	3	15:04
s04b2022.elem_min.txt	62734	May	3	15:04
s04b2022.elem_tot.txt	62747	May	3	15:04
s04c2204.6o	3663045	May	27	17:06
s04c2204.6p	40095	May	27	17:06
s04c2204.elem_aqu.txt	33447	May	27	17:06
s04c2204.elem_min.txt	31654	May	27	17:06
s04c2204.elem_tot.txt	31667	May	27	17:06
spwr.doc	946176	Aug	16	10:39
spwr00b.doc	710144	Sep	15	11:46
EXTERNAL.FNT	9900	Jun	1	17:41
HELP_PP	50724	Jun	1	17:42
PP.EXE	308609	Jun	1	17:41
PREFER.PP	57	Jun	1	17:42
Readme_no_U_glass.txt	503	Jun	1	17:28
data0.com	2302224	Jun	1	17:43
data0.nuc	2302224	Jun	1	17:43
s@1a1111.6i	44606	Jun	1	17:29
s@1a1111.6o	4158133	Jun	1	17:30
s@1a1111.bin	26298352	Jun	1	17:40
s@1a1111.elem_aqu.txt	40646	Jun	1	17:28
s@1a1111.elem_min.txt	38469	Jun	1	17:28
s@1a1111.elem_tot.txt	38482	Jun	1	17:28
s@1a1222.6i	44606	Jun	1	17:29
s@1a1222.6o	9014929	Jun	1	17:29
s@1a1222.bin	98836176	Jun	1	17:37
s@1a1222.elem_aqu.txt	82031	Jun	1	17:28
s@1a1222.elem_min.txt	77622	Jun	1	17:28
s@1a1222.elem_tot.txt	77635	Jun	1	17:28
test2.txt	433	Jun	23	21:13
test3.txt	296	Jun	22	15:51

ATTACHMENT III. CALCULATING REMAINING MASS

For each run, the mass remaining of a reactant (such as HLW glass) at any time can be calculated using (1) information provided by the 5th, 6th, and 7th digits of the file name (such as s01a*1111* for a single stage run, or s03a*2204*/s03b*2022* for a double stage run); (2) information provided in Table III-1; and (3) the following equation:

$$M_t = 5.807 * V * \rho * (m_i - rk * sk * (t - t_0))$$

where M_t is the mass remaining (kg) at time = t, 5.807 kg/g is a correction factor, which converts from a calculation based on one liter to a calculation based on the total void of a WP, V is the molar volume (cm^3/mol), ρ is the density (g/cm^3) of the reactant, m_i is the number of moles at time = 0, rk is the reaction rate (mol/cm^2·s), sk is the surface area (cm^2), t is the time (s), and t_0 is the starting time for the reactions, which is equal to zero for all reactants for all single-stage runs. The values of t_0 for double-stage runs are provided in Table III-2.

The file name gives reaction rate information. The 5th digit of the file name indicates the reaction rate of steel (indicated as "1" or "2," with the values listed in Table III-1). The 6th digit indicates the reaction rate of the HLW glass (indicated as "1" or "2," with the values listed in Table III-1, or "0" if the HLW glass has been consumed and the run is in stage 2 of a two-stage run). The 7th digit indicates the reaction rate of the SNF or fissile material (indicated as "1," "2," or "3" with the values listed in Table III-1, or "0" if the run is in stage 1 of a two-stage run and no SNF is involved in the reaction).

Table III-1 Kinetic input parameters for reaction path calculations

Reactant	Type of Reactant	*V* Molar Volume (cm^3/mol)	ρ Density (g/cm^3)	m_i Initial Moles	*Rk* Reaction Rate (mol/cm^2·s)			*sk* Surface Area (cm^2)
					1	2	3	
HLW glass	Glass	35.088	2.85	24.821	1.16E-15	3.47E-13	N/A	1915.1
SNF	SNF	5.803	7.98	0.00195	1.14E-15	2.28E-14	6.84E-13	0.443
304L HLW glass pour canister	Steel	6.870	7.94	11.705	4.61E-14	4.61E-13	N/A	150.80
A516 outer web	Steel	7.013	7.85	18.042	1.58E-11	4.52E-11	N/A	128.34
A516 impact plates	Steel	7.013	7.85	0.376	1.58E-11	4.52E-11	N/A	1.279
316L DOE SNF canister	Steel	6.938	7.98	1.614	4.57E-14	4.57E-13	N/A	23.216
304L_B_Poison	Steel	6.289	7.94	0.0212	4.61E-14	4.61E-13	N/A	3.062
Chrome plating	Steel	7.222	7.2	0.00108	4.61E-14	4.61E-13	N/A	3.062
316L basket	Steel	6.938	7.98	1.378	4.57E-14	4.57E-13	N/A	21.827

Table III-2. Starting Time for Double-Stage Runs.

Reactant	t_0 Starting Time (s) for Double-Stage Runs			
	Run s03b2022	Run s04b2022	Run s02g2021	Run s02g1021
HLW glass	0	0	0	0
SNF	1.39E+11	1.26E+11	6.39E+10	6.37E+10
304L HLW glass pour canister	0	0	0	0
A516 outer web	0	0	0	0
A516 impact plates	1.39E+11	1.26E+11	6.39E+10	6.37E+10
316L DOE SNF canister	1.39E+11	1.26E+11	6.39E+10	6.37E+10
304L_B_poison	1.39E+11	1.26E+11	6.39E+10	6.37E+10
Chrome plating	1.39E+11	1.26E+11	6.39E+10	6.37E+10
316L basket	1.39E+11	1.26E+11	6.39E+10	6.37E+10

Figure III-1 is a log-log plot of mass remaining for all components versus time for the single stage run s01a1111 calculated using the equation provided above. For example, the HLW glass remaining after 100,000 years (3.15E+12 s) was calculated using the equation above (using the reaction rates equal to "1," as provided in Table III-1, and t_0 equal to zero) and found to be 10,350 kg. When calculating the mass remaining for a double-stage run, if $t - t_0$ is a negative value, then the second stage has not begun yet and the mass remaining for that reactant is equal to the starting mass.

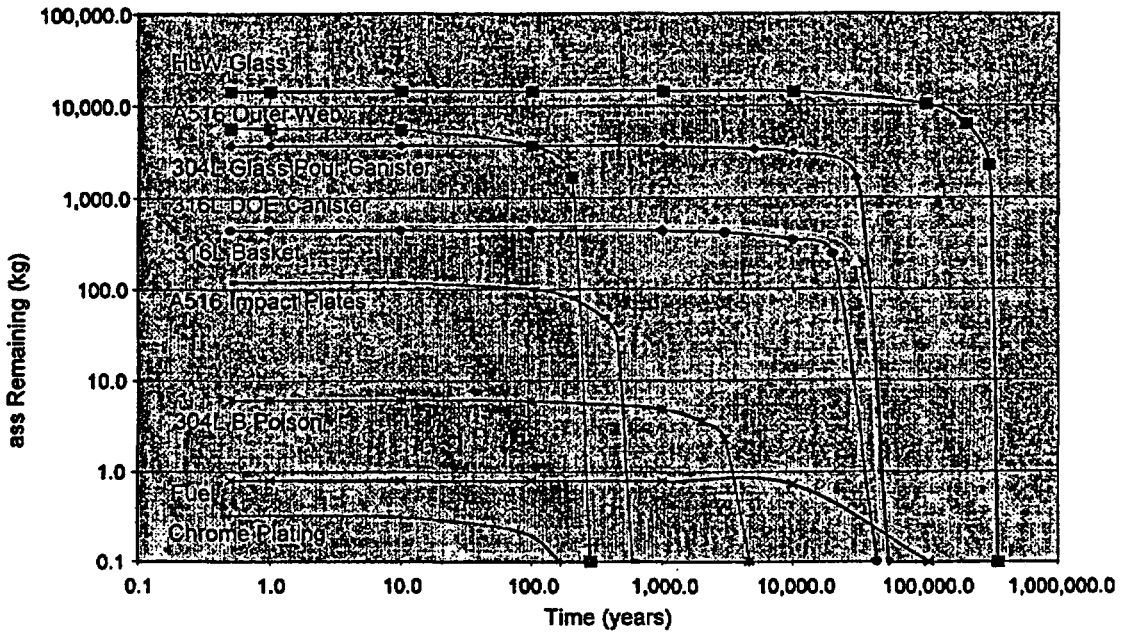

Figure III-1. Mass Remaining Versus Time for Case s01a1111

ATTACHMENT IV. DOCUMENT INPUT REFERENCE SHEETS

OFFICE OF CIVILIAN RADIOACTIVE WASTE MANAGEMENT
DOCUMENT INPUT REFERENCE SYSTEM

1. Document Identifier No./Rev.:	Change:	Title:
CAL-EDC-MD-000002 REV 00	N/A	EQ6 CALCULATION FOR CHEMICAL DEGRADATION OF SHIPPINGPORT PWR (HEU OXIDE) SPENT NUCLEAR FUEL WASTE PACKAGES

Input Document			4. Input Status	5. Section Used In	6. Input Description	7. TBV/TBD Priority	8. TBVDue To		
2a.	2. Technical Product Input Source Title and Identifier(s) with Version	3. Section					Unqual.	From Uncontrolled Source	Un-Confirmed
1	DOE (U.S. Department of Energy) 1999. *Shippingport PWR (HEU Oxide) Fuel Characteristics for Disposal Criticality Analysis.* DOE/SNF/REP-040, Revision 0. Washington, D.C.: U.S. Department of Energy. TIC: 243528.	3, Appendix C	TBV-3350	1, 5	Fuel description and composition	3	N/A	X	N/A
2	CRWMS M&O 1998. *EQ6 Calculations for Chemical Degradation of Fast Flux Test Facility (FFTF) Waste Packages.* BBA000000-01717-0210-00028 REV 00. Las Vegas, Nevada: CRWMS M&O. ACC: MOL.19981229.0081.	5.1.1.1, p. 203	TBV-3351	1, 5	VOID SPACE CALCULATION	3	X	N/A	N/A
3	CRWMS M&O 1998. "Disruptive Events." Chapter 10 of *Total System Performance Assessment-Viability Assessment (TSPA-VA) Analyses Technical Basis Document.* B00000000-01717-4301-00010 REV 00. Las Vegas, Nevada: CRWMS M&O. ACC: MOL.19980724.0399.	10.5.1.2	N/A - Reference Only	1, 5	Discussion of degradation scenarios	N/A	N/A	N/A	N/A

ATTACHMENT IV. DOCUMENT INPUT REFERENCE SHEETS

OFFICE OF CIVILIAN RADIOACTIVE WASTE MANAGEMENT
DOCUMENT INPUT REFERENCE SYSTEM

1. Document Identifier No./Rev.:	Change:	Title:
CAL-EDC-MD-000002 REV 00	N/A	EQ6 CALCULATION FOR CHEMICAL DEGRADATION OF SHIPPINGPORT PWR (HEU OXIDE) SPENT NUCLEAR FUEL WASTE PACKAGES

Input Document							8. TBVDue To		
2a.	2. Technical Product Input Source Title and Identifier(s) with Version	3. Section	4. Input Status	5. Section Used In	6. Input Description	7. TBV/TBD Priority	Unqual.	From Uncontrolled Source	Un-Confirmed
4	CRWMS M&O 1998. *Evaluation of Codisposal Viability for Aluminum-Clad DOE-Owned Spent Fuel: Phase II Degraded Codisposal Waste Package Internal Criticality.* BBA000000-01717-5705-00017 REV 01. Las Vegas, Nevada: CRWMS M&O. ACC: MOL.19981014.0038.	Entire	N/A - Reference Only	1	Discussion of codisposal concept	N/A	N/A	N/A	N/A
5	National Research Council 1995. *Technical Bases for Yucca Mountain Standards.* Washington, D.C.: National Academy Press. TIC: 217588.	Entire	N/A - Reference Only	1	Discussion of time fram for calculations	N/A	N/A	N/A	N/A
6	Harrar, J.E.; Carley, J.F.; Isherwood, W.F.; and Raber, E. 1990. *Report of the Committee to Review the Use of J-13 Well Water in Nevada Nuclear Waste Storage Investigations.* UCID-21867. Livermore, California: Lawrence Livermore National Laboratory. ACC: NNA.19910131.0274.	Tables 4.1 and 4.2	TBV-3352		DESCRIPTION OF J-13 WATER	3	X	N/A	N/A

ATTACHMENT IV. DOCUMENT INPUT REFERENCE SHEETS

OFFICE OF CIVILIAN RADIOACTIVE WASTE MANAGEMENT
DOCUMENT INPUT REFERENCE SYSTEM

1. Document Identifier No./Rev.:	Change:	Title:
CAL-EDC-MD-000002 REV 00	N/A	EQ6 CALCULATION FOR CHEMICAL DEGRADATION OF SHIPPINGPORT PWR (HEU OXIDE) SPENT NUCLEAR FUEL WASTE PACKAGES

Input Document			4. Input Status	5. Section Used in	6. Input Description	7. TBV/TBD Priority	8. TBVDue To		
2a.	2. Technical Product Input Source Title and Identifier(s) with Version	3. Section					Unqual.	From Uncontrolled Source	Un-Confirmed
7	DOE (U.S. Department of Energy) 1998. *Total System Performance Assessment.* Volume 3 of *Viability Assessment of a Repository at Yucca Mountain.* DOE/RW-0508. Washington, D.C.: U.S. Department of Energy, Office of Civilian Radioactive Waste Management. ACC: MOL.19981007.0030.	Secs. 3.5 to 3.6	N/A - Reference Only	3	Discussion of the role of mobile colloids in radionuclide transport from WP	N/A	N/A	N/A	N/A
		Fig. 3-20 to 3-22	N/A - Reference Only	3	Discussion of temperature at which initial breach of WP will occur	N/A	N/A	N/A	N/A
		p. 3-84	N/A - Reference Only	3	Discussion of role of microbiologically influenced corrosion on WP degradation	N/A	N/A	N/A	N/A
8	Yang, I.C.; Rattray, G.W.; and Yu, P. 1996. *Interpretation of Chemical and Isotopic Data from Boreholes in the Unsaturated Zone at Yucca Mountain, Nevada.* Water-Resources Investigations Report 96-4058. Denver, Colorado: U.S. Geological Survey. ACC: MOL.19980528.0216.	Table 8	N/A - Reference Only	3	Basis for using high partial pressure of carbon dioxide gas in calculations	N/A	N/A	N/A	N/A
9	Weast, R.C. 1977. *CRC Handbook of Chemistry and Physics. 58th Edition.* Pages B-121 and F-210. Cleveland, Ohio: CRC Press. TIC: 242376.	p. F-210	N/A - Accepted Data (Fact)	3.9	Value of carbon dioxide partial pressure in atmosphere	N/A	N/A	N/A	N/A
		p. B-121	N/A - Accepted Data (Fact)	5.1.1.5	value of density of hematite	N/A	N/A	N/A	N/A

ATTACHMENT IV. DOCUMENT INPUT REFERENCE SHEETS

OFFICE OF CIVILIAN RADIOACTIVE WASTE MANAGEMENT
DOCUMENT INPUT REFERENCE SYSTEM

1. Document Identifier No./Rev.:	Change:	Title:
CAL-EDC-MD-000002 REV 00	N/A	EQ6 CALCULATION FOR CHEMICAL DEGRADATION OF SHIPPINGPORT PWR (HEU OXIDE) SPENT NUCLEAR FUEL WASTE PACKAGES

Input Document			4. Input Status	5. Section Used In	6. Input Description	7. TBV/TBD Priority	8. TBVDue To		
2a.	2. Technical Product Input Source Title and Identifier(s) with Version	3. Section					Unqual.	From Uncontrolled Source	Un-Confirmed
10	CRWMS M&O 1996. *Second Waste Package Probabilistic Criticality Analysis: Generation and Evaluation of Internal Criticality Configurations.* BBA000000-01717-2200-00005 REV 00. Las Vegas, Nevada: CRWMS M&O. ACC: MOL.19960924.0193.	Attachment 6	N/A - Reference Only	3	Basis for assumption of convective circulation and mixing of water inside the WP	N/A	N/A	N/A	N/A
11	Hillner, E.; Franklin, D.G.; and Smee, J.D. 1998. *The Corrosion of Zircaloy-Clad Fuel Assemblies in a Geologic Repository Environment.* WAPD-T-3173. West Mifflin, Pennsylvania: Bettis Atomic Power Laboratory. TIC: 237127.	Entire	TBV-3353	3.18	ZIRCALOY AND ZR CORROSION KINETICS OF FUEL CLADDING	3	N/A	X	N/A
12	CRWMS M&O 1999. *Addendum to: EQ6 Computer Program for Theoretical Manual, Users Guide, & Related Documentation.* Software Change Request (SCR) LSCR198. UCRL-MA-110662 PT IV. Las Vegas, Nevada: CRWMS M&O. ACC: MOL.19990305.0112.	Entire	N/A - Reference Only	4	Software change request	N/A	N/A	N/A	N/A

ATTACHMENT IV. DOCUMENT INPUT REFERENCE SHEETS

OFFICE OF CIVILIAN RADIOACTIVE WASTE MANAGEMENT
DOCUMENT INPUT REFERENCE SYSTEM

1. Document Identifier No./Rev.:	Change:	Title:
CAL-EDC-MD-000002 REV 00	N/A	EQ6 CALCULATION FOR CHEMICAL DEGRADATION OF SHIPPINGPORT PWR (HEU OXIDE) SPENT NUCLEAR FUEL WASTE PACKAGES

Input Document							8. TBVDue To		
2a.	2. Technical Product Input Source Title and Identifier(s) with Version	3. Section	4. Input Status	5. Section Used In	6. Input Description	7. TBV/TBD Priority	Unqual.	From Uncontrolled Source	Un-Confirmed
13	CRWMS M&O 1998. *Software Qualification Report (SQR) Addendum to Existing LLNL Document UCRL-MA-110662 PT IV: Implementation of a Solid-Centered Flow-Through Mode for EQ6 Version 7.2b.* CSCI: UCRL-MA-110662 V 7.2B, SCR: LSR198, MI: 30084-M04-001 (Addendum Only). Las Vegas, Nevada: CRWMS M&O. ACC: MOL.19981214.0108.	Entire	N/A - Reference Only	4	Software Qualification Report	N/A	N/A	N/A	N/A
14	CRWMS M&O 1998. *EQ6 Calculations for Chemical Degradation of Pu-Ceramic Waste Packages.* BBA000000-01717-0210-00018 REV 00. Las Vegas, Nevada: CRWMS M&O. ACC: MOL.19980918.0004.	Entire	N/A - Reference Only	4	Describes allpost/nxtinput method	N/A	N/A	N/A	N/A
15	CRWMS M&O 1998. *EQ3/6 Software Installation and Testing Report for Pentium Based Personal Computers (PCs).* CSCI: LLYMP9602100. Las Vegas, Nevada: CRWMS M&O. ACC: MOL.19980813.0191.	Entire	N/A - Reference Only	4	Documentation of installation and test report for EQ3/6 software	N/A	N/A	N/A	N/A
16	Wolery, T.J. 1992. *EQ3/6, A Software Package for Geochemical Modeling of Aqueous Systems. Package Overview and Installation Guide (Version 7.0).* UCRL-MA-110662 PT I. Livermore, California: Lawrence Livermore National Laboratory. TIC: 205087.	Entire	N/A - Reference Only	3	Justification for using existing database supplied with EQ3/6	N/A	N/A	N/A	N/A
		Entire	N/A - Reference Only	3	Discussion of EQ3/6 Software	N/A	N/A	N/A	N/A

ATTACHMENT IV. DOCUMENT INPUT REFERENCE SHEETS

OFFICE OF CIVILIAN RADIOACTIVE WASTE MANAGEMENT
DOCUMENT INPUT REFERENCE SYSTEM

1. Document Identifier No./Rev.:	Change:	Title:
CAL-EDC-MD-000002 REV 00	N/A	EQ6 CALCULATION FOR CHEMICAL DEGRADATION OF SHIPPINGPORT PWR (HEU OXIDE) SPENT NUCLEAR FUEL WASTE PACKAGES

Input Document			4. Input Status	5. Section Used in	6. Input Description	7. TBV/TBD Priority	8. TBVDue To		
2a.	2. Technical Product Input Source Title and Identifier(s) with Version	3. Section					Unqual.	From Uncontrolled Source	Un-Confirmed
17	Daveler, S.A. and Wolery, T.J. 1992. *EQPT, A Data File Preprocessor for the EQ3/6 Software Package. User's Guide, and Related Documentation (Version 7.0).* UCRL-MA-110662 PT II. Livermore, California: Lawrence Livermore National Laboratory. TIC: 205240.	Entire	N/A - Reference Only	3	Justification for using existing databse supplied with EQ3/6	N/A	N/A	N/A	N/A
		Entire	N/A - Reference Only	4	Discussion of EQ3/6 Software	N/A	N/A	N/A	N/A
18	Wolery, T.J. 1992. *EQ3NR, A Computer Program for Geochemical Aqueous Speciation-Solubility Calculations. Theoretical Manual, User's Guide, and Related Documentation (Version 7.0).* UCRL-MA-110662 PT III. Livermore, California: Lawrence Livermore National Laboratory. TIC: 205154.	Entire	N/A - Reference Only	3, 4	Discussion of EQ3/6 Software	N/A	N/A	N/A	N/A
19	Wolery, T.J. and Daveler, S.A. 1992. *EQ6, A Computer Program for Reaction Path Modeling of Aqueous Geochemical Systems: Theoretical Manual, User's Guide, and Related Documentation (Version 7.0).* UCRL-MA-110662 PT IV. Livermore, California: Lawrence Livermore National Laboratory. TIC: 205002.	Entire	N/A - Reference Only	3, 4	Discussion of EQ3/6 Software	N/A	N/A	N/A	N/A

ATTACHMENT IV. DOCUMENT INPUT REFERENCE SHEETS

OFFICE OF CIVILIAN RADIOACTIVE WASTE MANAGEMENT
DOCUMENT INPUT REFERENCE SYSTEM

1. Document Identifier No./Rev.:	Change:	Title:
CAL-EDC-MD-000002 REV 00	N/A	EQ6 CALCULATION FOR CHEMICAL DEGRADATION OF SHIPPINGPORT PWR (HEU OXIDE) SPENT NUCLEAR FUEL WASTE PACKAGES

Input Document			4. Input Status	5. Section Used in	6. Input Description	7. TBV/TBD Priority	8. TBVDue To		
2a.	2. Technical Product Input Source Title and Identifier(s) with Version	3. Section					Unqual.	From Uncontrolled Source	Un-Confirmed
20	Spahiu, K. and Bruno, J. 1995. *A Selected Thermodynamic Database for REE to be Used in HLNW Performance Assessment Exercises.* SKB Technical Report 95-35. Stockholm, Sweden: Swedish Nuclear Fuel and Waste Management Company. TIC: 225493.	Entire	TBV-3354	3	JUSTIFICATION FOR USING EXISTING DATABASE SUPPLIED WITH EQ3/6	3	N/A	X	N/A
21	CRWMS M&O 1999. *Electronic Media (CD): The Calculation Files for EQ6 Calculation for Chemical Degradation of Shippingport PWR Spent Nuclear Fuel Waste Packages, CAL-EDC-MD-000002 REV 00.* Las Vegas, Nevada: CRWMS M&O. ACC: MOL.19991118.0179.	Entire	TBV-3355	3, 4, 5	EQ6 DATABASE FILES, GEOMETRY CALCULATIONS FOR SNF, WP, SOFTWARE ROUTINES	3	X	N/A	N/A
22	CRWMS M&O 1998. *EQ6 Calculations for Chemical Degradation of PWR LEU and PWR MOX Spent Fuel Waste Packages.* BBA000000-01717-0210-00009 REV 00. Las Vegas, Nevada: CRWMS M&O. ACC: MOL.19980701.0483.	4; 5.1.13	TBV-3356	4; 5	PROCEDURE FOR CALCULATION; PERCOLATION AND DRIP RATES	3	X	N/A	N/A
23	CRWMS M&O 1997. *Criticality Evaluation of Degraded Internal Configurations for the PWR AUCF WP Designs.* BBA000000-01717-0200-00056 REV 00. Las Vegas, Nevada: CRWMS M&O. ACC: MOL.19971231.0251.	p. 11-13	TBV-3357	5	STAINLESS STEEL DEGRADATION RATES	3	X	N/A	N/A

ATTACHMENT IV. DOCUMENT INPUT REFERENCE SHEETS

OFFICE OF CIVILIAN RADIOACTIVE WASTE MANAGEMENT
DOCUMENT INPUT REFERENCE SYSTEM

1. Document Identifier No./Rev.:	Change:	Title:
CAL-EDC-MD-000002 REV 00	N/A	EQ6 CALCULATION FOR CHEMICAL DEGRADATION OF SHIPPINGPORT PWR (HEU OXIDE) SPENT NUCLEAR FUEL WASTE PACKAGES

Input Document							8. TBVDue To		
2a.	2. Technical Product Input Source Title and Identifier(s) with Version	3. Section	4. Input Status	5. Section Used In	6. Input Description	7. TBV/TBD Priority	Unqual.	From Uncontrolled Source	Un-Confirmed
24	CRWMS M&O 1999. *DOE SRS HLW Glass Chemical Composition.* BBA000000-01717-0210-00038 REV 00. Las Vegas, Nevada: CRWMS M&O. ACC: MOL.19990215.0397.	Attachment 1, p. 1-7	TBV-3145	p;	*Chemical Composition of HLW* Glass. This reference uses existing preliminary data from "Preliminary Waste Form Characteristics Report" ACC: MOL.19940726.0118; Molar composition of HLW glass	3	X	N/A	N/A
25	DOE (U.S. Department of Energy) 1992. *Characteristics of Potential Repository Wastes.* DOE/RW-0184-R1. Volume 1. Washington, D.C.: U.S. Department of Energy, Office of Civilian Radioactive Waste Management. ACC: HQO.19920827.0001.	p. 3.3-15, Tab 3.3.8	N/A - Reference Only	p;	Discussion of HLW glass composition (used for comparison only, not as a numeric input)	N/A	N/A	N/A	N/A
26	CRWMS M&O 1995. *Total System Performance Assessment - 1995: An Evaluation of the Potential Yucca Mountain Repository.* B00000000-01717-2200-00136 REV 01. Las Vegas, Nevada: CRWMS M&O. ACC: MOL.19960724.0188.	Fig. 5.4-3, 4 & 5	TBV-3358	5	CARBON STEEL DEGRADATION RATE; GLASS DEGRADATION RATE	3	X	N/A	N/A
		p. 6.5, Fig. 6.2-5	TBV-3358		CARBON STEEL DEGRADATION RATE; GLASS DEGRADATION RATE	3	X	N/A	N/A
27	CRWMS M&O 1998. "Near-Field Geochemical Environment." Chapter 4 of *Total System Performance Assessment-Viability Assessment (TSPA-VA) Analyses Technical Basis Document.*	Fig. 4-27	TBV-3359	5	EQ3NR INPUT FILE CONSTRAINTS AND EQ6 INPUT FILE ELEMENTAL MOLAL COMPOSITIONS OF	3	X	N/A	N/A

ATTACHMENT IV. DOCUMENT INPUT REFERENCE SHEETS

OFFICE OF CIVILIAN RADIOACTIVE WASTE MANAGEMENT
DOCUMENT INPUT REFERENCE SYSTEM

1. Document Identifier No./Rev.:	Change:	Title:
CAL-EDC-MD-000002 REV 00	N/A	EQ6 CALCULATION FOR CHEMICAL DEGRADATION OF SHIPPINGPORT PWR (HEU OXIDE) SPENT NUCLEAR FUEL WASTE PACKAGES

Input Document			4. Input Status	5. Section Used In	6. Input Description	7. TBV/TBD Priority	8. TBVDue To		
2a.	2. Technical Product Input Source Title and Identifier(s) with Version	3. Section					Unqual.	From Uncontrolled Source	Un-Confirmed
	B00000000-01717-4301-00004 REV 01. Las Vegas, Nevada: CRWMS M&O. ACC: MOL.19981008.0004.				J-13 WATER				
28	CRWMS M&O 1998. *Complete Draft VA UZ Abstraction/Test Document.* B00000000-01717-2200-00201. Las Vegas, Nevada: CRWMS M&O. ACC: MOL.19980428.0202.	Figure 2.3-110	TBV-3360	5	CORRELATION BETWEEN PERCOLATION RATE AND DRIP RATE	3	X	N/A	N/A
		Table 2.3-49 & 50	TBV-3360	5	CORRELATION BETWEEN PERCOLATION RATE AND DRIP RATE	3	X	N/A	N/A
29	CRWMS M&O 1996. *Status Report on Degraded Mode Criticality Analysis of Immobilized Plutonium Waste Forms in a Geologic Repository.* A00000000-01717-5705-00013 REV 00. Vienna, Virginia: CRWMS M&O. ACC: MOL.19970324.0023.	p. 28	N/A - Reference Only	5	Discussion for highest removal of elements from WPs codisposed with glass	N/A	N/A	N/A	N/A
30	CRWMS M&O 1997. *Degraded Mode Criticality Analysis of Immobilized Plutonium Waste Forms in a Geologic Repository.* Predecisional Document. A00000000-01717-5705-00014 REV 01. Las Vegas, Nevada: CRWMS M&O. ACC: MOL.19980422.0911.	5.3, p. 5-19	N/A - Reference Only	5	Discussion for highest removal of elements from WPs codisposed with glass	N/A	N/A	N/A	N/A

ATTACHMENT IV. DOCUMENT INPUT REFERENCE SHEETS

OFFICE OF CIVILIAN RADIOACTIVE WASTE MANAGEMENT
DOCUMENT INPUT REFERENCE SYSTEM

1. Document Identifier No./Rev.:	Change:	Title:
CAL-EDC-MD-000002 REV 00	N/A	EQ6 CALCULATION FOR CHEMICAL DEGRADATION OF SHIPPINGPORT PWR (HEU OXIDE) SPENT NUCLEAR FUEL WASTE PACKAGES

Input Document			4. Input Status	5. Section Used In	6. Input Description	7. TBV/TBD Priority	8. TBVDue To		
2a.	2. Technical Product Input Source Title and Identifier(s) with Version	3. Section					Unqual.	From Uncontrolled Source	Un-Confirmed
31	Roberts, W.L.; Rapp, G.R., Jr.; and Weber, J. 1974. *Encyclopedia of Minerals.* Pages 172, 240, 241, 413, 500, 689, and 690. New York, New York: Van Nostrand Reinhold. TIC: 238571.	p. 172	N/A - Accepted Data (Fact)	5	Density of diaspore and pyrolusite	N/A	N/A	N/A	N/A
32	CRWMS M&O 1996. *Material Compositions and Number Densities for Neutronics Calculations.* BBA000000-01717-0200-00002 REV 00. Las Vegas, Nevada: CRWMS M&O. ACC: MOL.19960624.0023.	pp. 29-31	N/A - Accepted Data (Fact)	5	Atomic weights	N/A	N/A	N/A	N/A
33	Walker, F.W.; Parrington, J.R.; and Feiner, F. 1989. *Nuclides and Isotopes, Fourteenth Edition: Chart of the Nuclides.* San Jose, California: General Electric Company. TIC: 201637.	p. 50	N/A - Accepted Data (Fact)	5	Atomic weights	N/A	N/A	N/A	N/A
34	CRWMS M&O 1998. *Disposal Criticality Analysis Methodology Topical Report.* B00000000-01717-5705-00095 REV 00. Las Vegas, Nevada: CRWMS M&O. ACC: MOL.19980918.0005.	pp. 3-9 to 3-12	N/A - Reference Only	5	Degradation scenarios for disposal criticality analysis	N/A	N/A	N/A	N/A